Plant Pathology

WILEY

ORIGINAL ARTICLE OPEN ACCESS

Four Novel *Colletotrichum* Species Associated With Anthracnose of Ornamental Araceae in Brazil With Insights Into Their Host Range

Caio Mattos Pereira | Robert Weingart Barreto

Departamento de Fitopatologia, Universidade Federal de Viçosa, Viçosa, Minas Gerais, Brazil

Correspondence: Robert Weingart Barreto (rbarreto@ufv.br)

Received: 11 January 2026 | **Revised:** 24 March 2026 | **Accepted:** 16 April 2026

Keywords: aroids | cross-inoculations | cut-flower industry | host-range | leaf spots | novel pathogens | phylogeny

ABSTRACT

Araceae includes numerous flowering plant species that are cultivated as ornamentals in gardens, pots or by the cut-flower industry. Relatively little has been published on the fungal pathogens attacking these ornamentals, particularly in Brazil. Here we report the results of a study on *Colletotrichum* spp. found in association with anthracnose and leaf spot symptoms on *Aglaonema commutatum*, *Anthurium andraeanum*, *Dieffenbachia amoena*, *Philodendron imbe* and *Philodendron tripartitum*. Nine isolates of *Colletotrichum* were obtained from diseased tissues. A polyphasic approach was used to identify these isolates as four novel species: *Colletotrichum anthuriicola* sp. nov., *C. araceiphilum* sp. nov., *C. imbeicola* sp. nov. and *C. philodendrifolium* sp. nov. Cross-inoculation assays were conducted using the plant host species listed above, as well as *Epipremnum aureum*, and showed that all isolates were pathogenic to at least three of the inoculated aroid species. These findings expand the current knowledge of the genus *Colletotrichum* and its association with members of the Araceae and highlight the need to consider individual ornamental aroids as potential inoculum reservoirs for infection of other cultivated members, given the low host specificity of aroid-associated *Colletotrichum* species.

1 | Introduction

Ornamental plants are the most diverse group of cultivated plants and are of great economic importance worldwide (Lecomte et al. 2016). The global market value of ornamentals is expected to reach $45 billion by 2029 (Data Bridge Market Research [DBMR] 2025). Paradoxically, compared with other crops, diseases of ornamentals have been relatively under-investigated. This gap poses a threat to the ornamental plant sector, which is constrained by the occurrence of destructive diseases (Zhang, Nizamani, et al. 2023).

Ornamentals of the family Araceae exemplify this broader lack of basic phytopathological knowledge. Although plant diseases are known to negatively impact their production and quality, and some studies—including a few from our research group (Pereira et al. 2024; Visagie et al. 2024)—have addressed diseases affecting aroids, the pathogens associated with these hosts remain poorly documented and insufficiently investigated.

As aroids are commonly propagated vegetatively under shaded and very humid conditions, fungal diseases such as anthracnose may have a significant impact on their production for the cut flower industry (particularly anthurium and arum lily) (Chaves et al. 2020; Norman and Ali 2012), for the potted plants market (such as anthurium, Chinese evergreen and dumbcane) (de Álvarez and Álvarez 2001; Chaudhuri et al. 2018), and for cultivation in gardens (numerous varieties) (Cui et al. 2025; Liu et al. 2021; Vásquez-López et al. 2019).

Colletotrichum, discovered by Corda (1831), is the only genus in the Glomerellaceae (Liu et al. 2022). It has long been

This is an open access article under the terms of the Creative Commons Attribution License, which permits use, distribution and reproduction in any medium, provided the original work is properly cited.

© 2026 The Author(s). *Plant Pathology* published by John Wiley & Sons Ltd on behalf of British Society for Plant Pathology.

considered one of the most important genera of fungal plant pathogens (Dean et al. 2012) and is widely regarded as the aetiological agent of anthracnoses. Nevertheless, it can also cause leaf spots, stem blight and fruit rots on a wide range of hosts, both in tropical and temperate regions (Talhinhas and Baroncelli 2021; Zhang, Nizamani, et al. 2023). Members of *Colletotrichum* spp. also occupy other ecological niches, including lifestyles as endophytes, saprophytes and even insect pathogens (Jayawardena et al. 2020). The genus comprises more than 340 accepted species, now mostly circumscribed through molecular data. It has been organised into 16 species complexes by Liu et al. (2022) and was expanded to include four additional complexes later proposed by Talhinhas and Baroncelli (2023). Modern reappraisals of *Colletotrichum* (based on the use of molecular tools) have dramatically changed the taxonomy for the genus (e.g., Bhunjun et al. 2021; Damm et al. 2019).

In the past, *Colletotrichum* species were described solely based on morphological, cultural characteristics and supposed host-specificity. This was inadequate due to overlapping characteristics between taxa (Zhang, Chen, et al. 2023). Thus, accurate species delimitation based on a polyphasic approach is essential for the proper characterisation of mycodiversity, for understanding pathogen–host interactions and evolutionary dynamics, and for supporting the development of effective management strategies for *Colletotrichum* diseases (Liu et al. 2022).

This study represents the first application of the polyphasic approach to investigate the taxonomy of *Colletotrichum* species associated with ornamental Araceae in Brazil. Although the sampling was largely confined to a single plant nursery, it provides an initial step towards a broader understanding of the fungi responsible for anthracnose of aroids.

2 | Materials and Methods

2.1 | Sampling and Fungal Isolation

The following ornamental Araceae species were studied here: *Aglaonema commutatum*, common name Chinese evergreen or poison dart (*café-de-salão* in Brazil), *Anthurium andraeanum*, common name flamingo flower (*antúrio* in Brazil), *Dieffenbachia amoena*, common name dumbcane (*comigo-ninguém-pode* in Brazil), *Epipremnum aureum*, common name golden pothos (*jiboia* in Brazil), *Philodendron imbe*, no common English name (*imbê* in Brazil), *Philodendron tripartitum*, common name three-lobed philodendron (*filodendro tripartido* in Brazil) and *Syngonium podophyllum*, common name arrowhead plant (*singônio* in Brazil).

Sampling occurred in the main ornamental plant nursery supplying plants for cultivation in the gardens of the campus of the Universidade Federal de Viçosa (UFV), Viçosa, state of Minas Gerais (Brazil). Additionally, samples of one species (*Philodendron imbe*) were also collected from a private garden in the city of Rio de Janeiro, state of Rio de Janeiro (Brazil) (Figure 1A). Mature and young leaves of each Araceae species showing leaf spots (Figure 1B–H) were collected and transported to the laboratory for further examination.

Upon arrival, while still fresh, the leaves were examined under a dissecting microscope (SZX7, Olympus) for closer examination of lesions. As previously suspected, several of the leaf spots were associated with fungi belonging to *Colletotrichum*. The lesions were therefore examined for typical features of *Colletotrichum* spp., including acervuli, setae and conidial masses.

Whenever the presence of *Colletotrichum* structures was confirmed, conidia were either collected with a sterile needle and transferred onto potato dextrose agar (PDA) plates, or selected fragments were excised from the leaves and left for 15 min laying on the surface of tap water agar plates, in order to soften the conidial masses to facilitate conidial transfer. The plates were then left in an incubator for 5 days at 25°C ± 2°C, under a 12-h light regime. Pure cultures were obtained, and representative isolates were deposited in the culture collection 'Coleção Octávio de Almeida Drumond' (COAD) of the UFV (Table S1). Additionally, selected leaves bearing sporulating lesions were dried in a plant press and deposited in the UFV fungarium (VIC).

2.2 | Morphological Analysis

An isolate obtained from each plant species was selected and transferred to oatmeal agar (OA), PDA and synthetic nutrient-poor agar (SNA) media, and maintained in an incubator for 7 days at 25°C ± 2°C in darkness. Colonies had their characteristics described following the terminology of Crous et al. (2019), and colour terminology followed Rayner's colour chart (Rayner 1970).

To assess biometric data and induce sporulation, a methodology adapted from Damm et al. (2012) was used. Autoclaved parsley stems (*Petroselinum crispum*, Apiaceae) were used in place of autoclaved stems of *Anthriscus sylvestris* (Apiaceae) and positioned on the surface of SNA plates. Each isolate was then transferred to the centre of an individual plate and incubated for 10 days at 25°C ± 2°C under a 12 h photoperiod. Appressoria were observed on slide cultures prepared as described by Johnston and Jones (1997), using SNA blocks as the starting point for *Colletotrichum* colony development. All slides, including slide cultures, were mounted in lactoglycerol and examined under a light microscope (BX-51; Olympus) equipped with a digital imaging system (Q-Colour 3 camera; Olympus). For each structure, 30 measurements were recorded following the protocol of Damm et al. (2012).

2.3 | DNA Extraction and Amplification

Isolates were grown on PDA for 10 days, under the same conditions described above. Mycelium was collected from the surface of the medium, transferred to a sterile 1.5 mL microcentrifuge tube containing three stainless steel beads, and ground using a mechanical cell disruptor (L-BEADER-3; Loccus Biotecnologia). The genomic DNA was extracted with the Wizard Genomic DNA Purification Kit (Promega), following the manufacturer's instructions.

Fragments from seven loci were targeted: actin (*act*), calmodulin (*cal*), chitin synthase 1 (*chs-1*), glyceraldehyde 3-phosphate

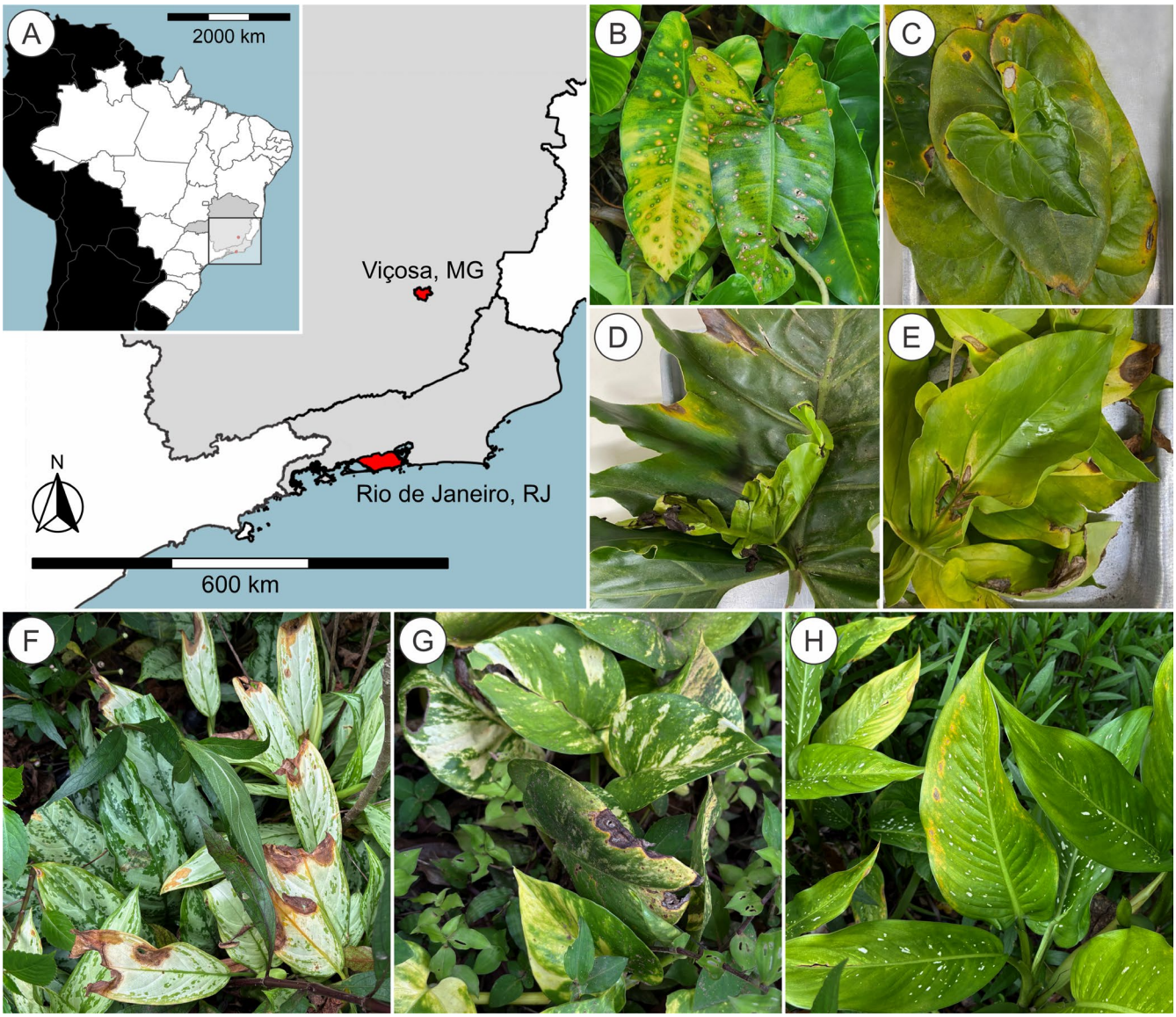


FIGURE 1 | Leaf spots on ornamental aroids in Brazil collected as possibly infected by *Colletotrichum* spp. (A) Localities of collection in Brazil. Symptoms on leaves of (B) *Philodendron imbe*—positive for *Colletotrichum* infection. (C) *Anthurium andraeanum*—positive for *Colletotrichum* infection. (D) *Philodendron tripartitum*—positive for *Colletotrichum infection*. (E) *Syngonium podophyllum*—negative for *Colletotrichum* infection (aetiology unresolved). (F) *Aglaonema commutatum*—positive for *Colletotrichum* infection. (G) *Epipremnum aureum*—negative for *Colletotrichum* infection (symptoms probably caused by the infection by *Cercospora* Q alone) and (H) *Dieffenbachia amoena*—positive for *Colletotrichum* infection.

dehydrogenase (*gapdh*), histone H3 (*his3*), the rDNA internal transcribed spacer region (ITS) and β-tubulin 2 (*tub2*). These were amplified using the primer pairs listed in Table S2. PCR conditions consisted of an initial denaturation step at 95°C for 5 min; followed by 35 cycles of 95°C for 30 s, annealing temperatures and times listed in Table S2, and 72°C for 45 s; and a final 72°C for 10 min.

To verify the purity and size of the amplicons, the PCR products were analysed on an agarose gel and visualised under UV light. Those showing amplification bands were purified using ExoSAP-IT (Amersham Biosciences) according to the manufacturer's instructions. DNA sequencing was carried out by Macrogen Inc. (Seoul, South Korea, http://www.macrogen.com).

2.4 | Phylogenetic Analysis

The results of sequencing were visualised and evaluated using the software SeqAssem v. 07/2008 (Hepperle 2021). The electropherograms were analysed and, when necessary, nucleotides on ambiguous positions were corrected. Consensus sequences were assembled, preliminarily compared with published sequences through a BLAST search (https://blast.ncbi.nlm.nih.gov/Blast.cgi) and deposited in GenBank (accession numbers are in Table S1).

Individual datasets were obtained through alignment of sequences of the isolates under study with other *Colletotrichum* sequences retrieved from Liu et al. 2022; Vieira et al. 2020; Xue et al. 2020; Zapata et al. 2024; Zhang, Chen, et al. 2023, and others available at the nucleotide NCBI database (Table S1).

The MUSCLE function of MEGA v. 10.2.2 software (Kumar et al. 2018) was applied to align these sequences. Then, SequenceMatrix v. 1.8 software (Vaidya et al. 2011) was used to generate a combined dataset of the seven loci. Phylogenetic analyses were performed within the CIPRES portal (Miller et al. 2010), using the maximum likelihood (ML) and the Bayesian inference (BI) methods.

To determine the species complexes to which the isolates belonged, an initial ML analysis was conducted using representative members of the *Colletotrichum* species complexes, with *Monilochaetes infuscans* CBS 869.96 designated as the outgroup (Figure S1). This analysis indicated that all isolates were clustered within the *Colletotrichum boninense* species complex. Accordingly, all members of this complex were included in the subsequent phylogenetic analyses. *Colletotrichum gloeosporioides* (CBS 112999 and CBS 953.97) was used the outgroup.

ML analysis was conducted using the RAxML-HPC v. 8.2.12 (Stamatakis 2014). The best phylogenetic tree was obtained after sampling 10,000 bootstrap replicates and bootstrap values (BS) > 70% were retained in the final tree.

Prior to the BI analysis, the best substitution model for each locus was determined through the ModelTest2 v. 2.1.6 tool (Darriba et al. 2012; also available on the CIPRES portal). The following substitution models were implemented in the BI analysis: for *act*, *gapdh* and *his3*, HKY + G; for *cal*, HKY + I; for *chs-1* and for *tub2*, K80 + G; and for ITS, K80 + I + G.

BI analysis was conducted using the MrBayes v. 3.2.1 tool (Ronquist et al. 2012). The Markov chain Monte Carlo (MCMC) method was used to find the best tree topology. Two simultaneous and independent analyses were conducted, each with four chains. The MCMCs were run for 5,000,000 generations, and trees were sampled every 500th generation, until convergence was achieved. The first 25% of trees were discarded in the burn-in phase, and the remaining 7500 trees from each run generated the consensus tree, from which posterior probability values (PP) were obtained. Only PPs values higher than 0.90 were maintained in the final tree.

Phylogenetic trees were viewed using TreeGraph 2 v. 2.15.0-887 software (Stöver and Müller 2010). Topologies derived from the ML and BI analyses were compared and found to be congruent. The BI topology was therefore selected for presentation, and BS values from the ML analysis were mapped on to the tree.

2.5 | Pairwise Homoplasy Index

To validate the taxonomic independence of proposed taxa, Genealogical Concordance Phylogenetic Species Recognition (GCPSR) analysis was applied. A pairwise homoplasy index (PHI) test (Φ_w) was conducted to detect recombination among the isolates under study and closely related taxa. The test was performed in SplitsTree v. 6.7.5 (Huson and Bryant 2024) using concatenated ITS, *gapdh*, *chs*, *act*, *tub2*, *his3* and *cal* sequences, and including ex-type strains of closely related taxa. A Φ_w value higher than 0.05 ($\Phi_w > 0.05$) indicated no significant recombination within the dataset (Bruen et al. 2006), suggesting a clear genetic separation among the analysed taxa. Relationships among closely related taxa were visualised using a NeighborNet network based on LogDet distances.

2.6 | Pathogenicity Tests

Pathogenicity tests were conducted to fulfil Koch's postulates with selected isolates of *Colletotrichum* obtained from the aroids during the survey. Ten healthy plants (approximately 6 months old) of *A. commutatum*, *A. andraeanum*, *D. amoena*, *E. aureum*, *P. imbe* and *P. tripartitum* were obtained from the ornamental plant nursery of UFV and used in the assays. *Epipremnum aureum* was included as an additional aroid species due to published reports of *Colletotrichum* spp. on this host in the United States and China (Hong Kong) (Farr et al. 2026). Two inoculation methods were used: (i) inoculation of intact foliage (without wounds), at five different spots on the middle of five separate leaves; and (ii) inoculation of five separate leaves, previously wounded using a cushion of sterile needles at five inoculation spots. Additionally, two kinds of inoculum were used: half of the plants received mycelium discs, while the other half was treated with conidial suspensions.

Isolates COAD 3509, COAD 3511, COAD 3513 and COAD 3514 were selected for pathogenicity tests as representatives of the four species identified within the isolate assemblage (see below). These were grown on either PDA plates or placed next to autoclaved parsley stems laying over the medium surface of SNA plates. Plates were maintained under the same conditions as described above. After 10 days, mycelium discs were taken from the margin of growing colonies (PDA plates). Conidial suspensions were prepared by transferring parsley stems colonised by *Colletotrichum* (and producing sporulating colonies) into plastic beakers containing 100 mL of an autoclaved Tween 0.05% (v/v) solution and blended with a homogeniser (model MA 102; Marconi). Each suspension was filtered through plastic sieves. Conidial concentrations were adjusted to 5×10^5 conidia/mL with a haemocytometer.

A cross-inoculation scheme was conducted. For each plant species, every possible combination of inoculum type (mycelium discs or conidial suspension) and inoculation method (with or without wounding) was tested for each isolate. This meant that one plant was treated per inoculum type, and individual leaves within each plant were considered as replicates for the inoculation method. Up to five mycelium discs were randomly placed on the adaxial surface of the leaves with the mycelium in direct contact with the leaf. On wounded leaves, up to five mycelium discs were placed directly over the wounds. Conidial suspensions were applied onto test plants either having intact or wounded leaves. The suspension was sprayed with hand-held atomisers until run-off occurred on each leaf. A set of plants (with and without wounding) received PDA discs from non-colonised plates or were sprayed with tap water and served as controls. After being treated, all plants were maintained in humidity chambers prepared by covering the plants and pots individually with large, wetted black plastic bags (100 L). A water-soaked paper pad was also placed at the base of each plant prior to closing each bag. The plants were kept under these

conditions for 72 h, after which the plastic bags were removed and the plants were transferred to greenhouse benches, where the air temperature was maintained at 25°C and the plants were watered twice a day. Plants were checked daily for the development of signs and/or symptoms. Symptomatic leaves were collected for examination under the dissecting microscope. Slides were mounted for microscopic observation of fungal structures found on sporulating lesions. When *Colletotrichum* was confirmed on samples, isolation was conducted following the procedures described above.

3 | Results

3.1 | Sampling and Fungal Isolation

The survey of anthracnosed aroids resulted in nine isolates of *Colletotrichum*. Four isolates were obtained from *Philodendron imbe* (COAD 3509, COAD 4218, COAD 4219 and COAD 4220), two isolates were obtained from *Philodendron tripartitum* (COAD 3512 and COAD 3513), and one isolate was obtained from each of the following hosts: *Anthurium andraeanum* (COAD 3511), *Aglaonema commutatum* (COAD 3514) and *Dieffenbachia amoena* (COAD 3515). *Epipremnum aureum* and *Syngonium podophyllum* did not yield any *Colletotrichum* isolates during the survey.

3.2 | Symptoms

Between 2022 and 2025, symptoms were frequently observed on leaves of the aroids cultivated at the ornamental plant nursery of UFV (Viçosa, Minas Gerais, Brazil), and in a private garden in Rio de Janeiro (Rio de Janeiro, Brazil). In the UFV nursery, all individuals of the five species exhibited anthracnose symptoms on many older leaves; similarly, *P. imbe* plants in the private garden also showed symptoms on older foliage.

On *A. commutatum*, early symptoms appeared as small, yellow to green spots, which progressed to form brown, oval lesions surrounded by yellow haloes, predominantly along leaf margins. Conidiomata were frequently visible on the adaxial leaf surface, and in advanced stages the necrotic parts of leaves often abscised, resulting in perforations.

On *A. andraeanum*, initial symptoms consisted of small brown spots surrounded by yellow haloes. These lesions expanded into oval to irregular, greyish and necrotic areas with dark brown margins and yellow halos and increased progressively in size leading, in some instances, particularly on plants directly exposed to the sun light, to the destructive and entire blight of many leaves of diseased plants. All sun-exposed plants showed leaf spots, which developed later into extensive leaf blight of older leaves.

On *D. amoena*, symptoms typically began as water-soaked yellow to green spots, progressing into greyish to brown with yellow haloes, round to oval lesions. In older lesions, conidiomata were commonly observed on the adaxial surface, and the necrotic tissue frequently detached, perforating the lesion centres.

On *P. imbe*, spots were numerous (particularly in plants growing at full sun compared to shaded plants) and affected large areas of the leaf surface, beginning as small yellow to green spots. Lesions expanded and sometimes coalesced, forming necrotic areas with greyish centres and brown margins surrounded by yellow haloes. Conidiomata were occasionally observed on the adaxial surface of older lesions.

On *P. tripartitum*, symptoms were predominantly observed along leaf margins and initially appeared as small and round brown spots. As the disease progressed, lesions coalesced and became sunken, necrotic, dark brown to black, surrounded by yellow haloes.

Although no *Colletotrichum* isolates were obtained from *E. aureum* or *S. podophyllum*, these hosts initially exhibited anthracnose-like symptoms in the form of small green to yellow spots that expanded and sometimes coalesced to form oval lesions with black to dark brown centres and yellow haloes.

3.3 | Phylogeny

Preliminary species identification, based on BLASTn search and ML analysis with members of all *Colletotrichum* species complexes, indicated that isolates belonged to the *Colletotrichum boninense* species complex (Figure S1).

The analysis of the *C. boninense* species complex comprised 99 isolates: 88 isolates from 43 described taxa, the nine isolates obtained in this study, and two isolates of *C. gloeosporioides* (CBS 953.97 and CBS 112999) used as outgroups. Phylogenetic relationships were inferred using a combined dataset of seven loci.

The final alignment consisted of 2221 characters, including gaps (ITS: 457, *gapdh*: 252, *chs-1*: 189, *act*: 220, *tub2*: 351, *his3*: 358, *cal*: 394), of which 1402 characters were conserved (ITS: 388, *gapdh*: 77, *chs-1*: 137, *act*: 106, *tub2*: 213, *his3*: 250, *cal*: 231), 808 characters were considered variable (ITS: 69, *gapdh*: 168, *chs-1*: 52, *act*: 114, *tub2*: 137, *his3*: 106, *cal*: 162) and 744 characters were parsimony-informative (ITS: 60, *gapdh*: 153, *chs-1*: 52, *act*: 105, *tub2*: 125, *his3*: 95, *cal*: 154).

The ML and BI analyses resulted in similar topologies; thus, the BI topology was selected and shown herein (Figure 2), with the BS values (obtained by the ML method) added.

COAD 3511 was closely related to *C. torulosum* in a group with high support values (BS = 96; ML = 1), but in a separate branch. The remaining three isolates (COAD 3512, COAD 3514 and COAD 3515) were grouped in a well-supported clade (BS = 79; ML = 1), phylogenetically related to *C. pseudoboninense*.

Four isolates (COAD 3509, COAD 4218, COAD 4219 and COAD 4220) formed a distinct and well-supported clade (BS = 100;

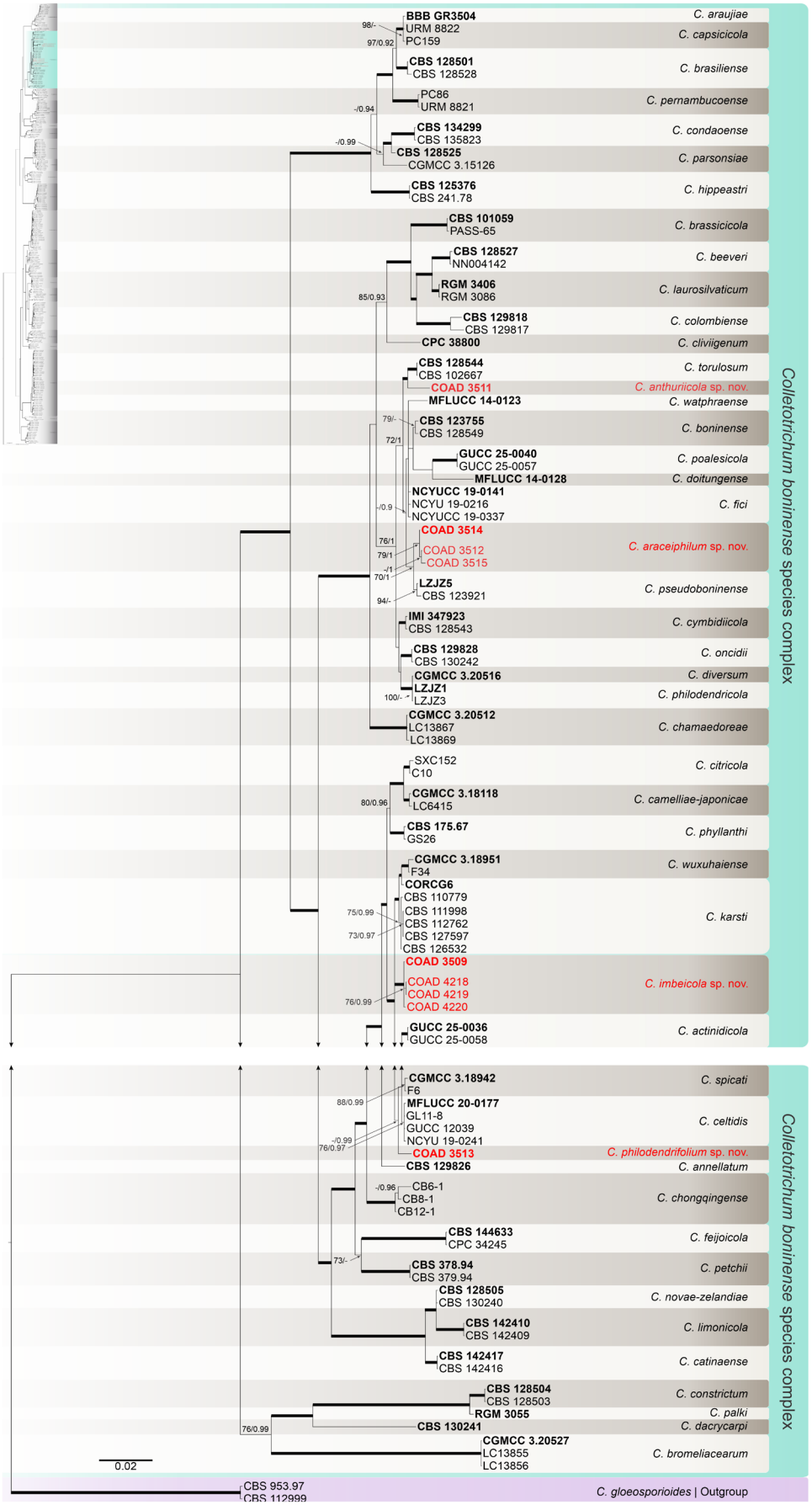


FIGURE 2 | Legend on next page.

FIGURE 2 | Phylogenetic tree based on Bayesian inference analysis (BI) and maximum-likelihood (ML) of the rDNA internal transcribed spacer region (ITS), glyceraldehyde 3-phosphate dehydrogenase (*gapdh*), chitin synthase 1 (*chs-1*), actin (*act*), β-tubulin 2 (*tub2*), histone H3 (*his3*) and calmodulin (*cal*) sequences of members of the *Colletotrichum boninense* species complex. Thickened branches indicate nodes with ML bootstrap support (BS) higher than 90% and BI posterior probabilities (PP) values higher than 0.95. Values at nodes indicate BS values (left, values ≥ 70%) and PP from BI (right, values ≥ 0.9). Lower values are indicated as '–'. The tree is rooted with *C. gloeosporioides* (CBS 112999 and CBS 953.97). Ex-type strains are highlighted in bold, and isolates treated in this study are presented in red.

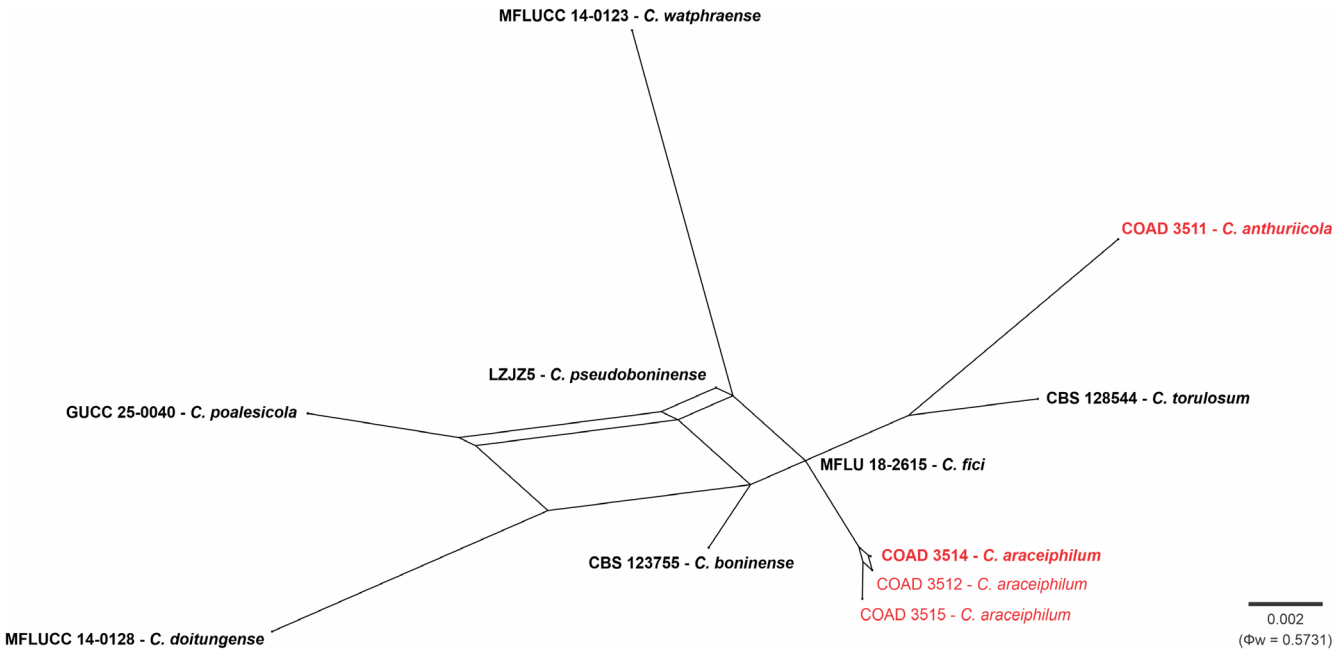


FIGURE 3 | Split graphs displaying the results of the pairwise homoplasy index (PHI) test of *Colletotrichum anthuricola* (COAD 3511) and *C. araceiphilum* (COAD 3512, COAD 3514 and COAD 3515) and their closely related taxa, inferred using a NeighborNet network based on LogDet distances from concatenated multilocus sequences. The PHI test result ($\Phi_w = 0.5731$) indicated that there is no evidence for significant recombination within the dataset. Ex-type strains are shown in bold and isolates of the new species are highlighted in red.

PP = 1) closely related to *C. karsti*, *C. wuxuhaiense*, *C. actinidicola*, *C. spicati*, *C. celtidis* and to the isolate COAD 3513. However, COAD 3513 was found to be more closely related to the latter three taxa, forming a distinct branch (BS = 48; PP = 0.99). Those nine isolates were assigned to four new species, which are described below.

To further validate these new species and their taxonomic independence, the GCPSR model was applied, and a PHI test based on seven concatenated loci was conducted to detect recombination events among phylogenetically closely related taxa. The PHI test indicated no significant recombination ($\Phi_w = 0.5731$) between *C. anthuriicola* (COAD 3511) and *C. araceiphilum* (COAD 3512, COAD 3514 and COAD 3515) and their closely related taxa, including *C. boninense*, *C. doitungense*, *C. fici*, *C. poalesicola*, *C. pseudoboninense*, *C. torulosum* and *C. watphraense* (Figure 3).

Similarly, the test resulted in a non-significant value ($\Phi_w = 0.3879$) and indicated no detectable recombination between *C. imbeicola* (COAD 3509, COAD 4218, COAD 4219 and COAD 4220) and *C. philodendrifolium* (COAD 3513) and their closely related species, including *C. actinidicola*, *C. celtidis*, *C. karsti*, *C. spicati* and *C. wuxuhaiense* (Figure 4). Therefore, these results support the genetic distinctiveness and independence of the newly proposed species.

3.4 | Taxonomy

3.4.1 | *Colletotrichum anthuriicola* sp. nov. C. M. Pereira & R. W. Barreto Figure 5

MycoBank: 861822.

Etymology: Based on the name of its host genus.

Typus: Brazil, Minas Gerais, Viçosa, on leaves of *Anthurium andraeanum* (Araceae), 20th Jul 2022, Robert W. Barreto (coll. number RWB 2398), holotype VIC 49390; ex-type living culture COAD 3511.

Description: *sexual morph* not observed. *Hyphae* hyaline to pale brown, smooth, septate, branched, 1.5–3.5 μm diam. *Conidiomata* acervular, scattered or in groups, black. *Setae* not observed. *Conidiophores* mostly reduced to conidiogenous cells, hyaline to pale brown, smooth, cylindrical, clavate, sometimes obclavate, straight, septate, unbranched, 7–15.5 × 3–4 μm ($\bar{x} = 11.3 \pm 3.3 \times 3.3 \pm 0.4$ μm), L/W ratio = 3.4. *Conidiogenous cells* mostly formed directly on mycelium, hyaline to pale brown, smooth, cylindrical to ampulliform, 8.5–29 × 2–4 μm ($\bar{x} = 18.8 \pm 5.4 \times 3 \pm 0.8$ μm), L/W ratio = 6.2. *Conidia* hyaline, aseptate, smooth, cylindrical, ellipsoid, occasionally obovoid,

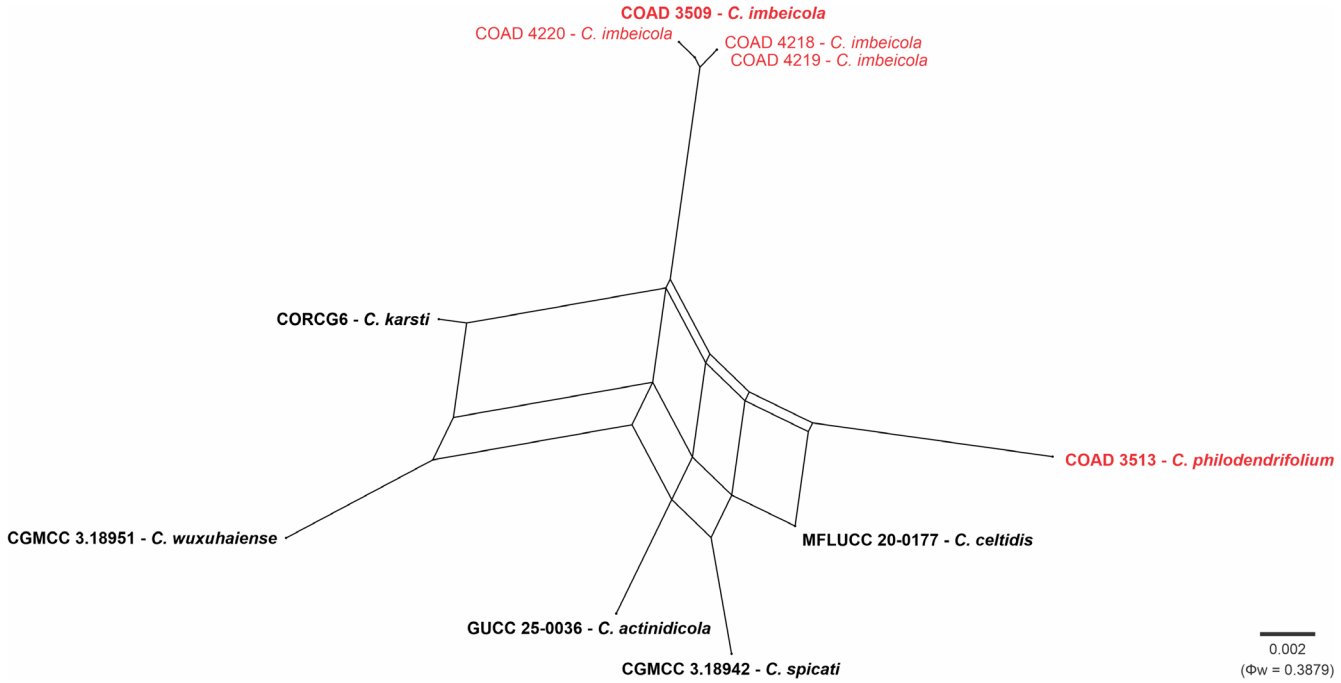


FIGURE 4 | Split graphs displaying the results of the pairwise homoplasy index (PHI) test of *Colletotrichum imbeicola* (COAD 3509, COAD 4218, COAD 4219, and COAD 4220) and *C. philodendrifolium* (COAD 3513) and their closely related taxa, inferred using a NeighborNet network based on LogDet distances from concatenated multilocus sequences. The PHI test result ($\Phi_w = 0.3879$) indicated that there is no evidence for significant recombination within the dataset. Ex-type strains are shown in bold, and isolates of the new species are highlighted in red.

rounded at both ends, occasionally tapering towards a subacute base, occasionally with a distinct hilum at base, 11.5–17.5 × 5–7 µm ($\bar{x}$ = 13.1 ± 3 × 5.9 ± 0.4 µm), L/W ratio = 2.2. *Appressoria* solitary, dark brown, smooth, ovoid, clavate or irregular with entire to undulate margins, 8–17 × 5–10 µm ($\bar{x}$ = 10.5 ± 1.7 × 7.7 ± 1 µm), L/W ratio = 1.4.

Culture characteristic: colonies on OA fast-growing 70 mm diam. after 7 days, flat, edge slightly undulate, aerial mycelium feathery, greenish olivaceous to grey olivaceous centrally with white margins; reverse greenish olivaceous with white margins. On PDA fast-growing 75 mm diam. after 7 days, flat, edge entire, aerial mycelium felty, lavender grey surrounded with white periphery; reverse olivaceous grey with white periphery. On SNA fast-growing, 66 mm diam. after 7 days, flat, edge slightly undulate, aerial mycelium feathery with some tufts, surface and reverse white. Sporulation absent on all media.

Notes: *C. anthuriicola* is represented in this study by a single isolate, that forms a close, yet distinct and well-supported (96/1) branch in relation to *C. torulosum*. Morphologically, these species are distinguishable by the size of conidiophores, which are shorter in *C. anthuriicola*—up to 15.5 µm long versus up to 75 µm long in *C. torulosum* (Damm et al. 2012) and by the length of conidiogenous cells, which are slightly longer in *C. anthuriicola* (up to 29 µm long) than in *C. torulosum* (up to 23 µm long) (Damm et al. 2012). *C. torulosum* has been reported in association with several hosts, although not with any aroid. Documented hosts include *Solanum melongena* (Solanaceae), *Passiflora edulis* (Passifloraceae) (Damm et al. 2012) and *Kunzea ericoides* (Myrtaceae) (Talhinhas and Baroncelli 2023), with all known records restricted to New Zealand.

Another *Colletotrichum* species, *C. anthurii*, was described in the 19th century from leaves of *Anthurium* sp. in France (Delacroix 1897). *C. anthuriicola* is clearly distinct as it produces conidia which are smaller (11.5–17.5 × 5–7 µm) and biometrically disjunct from those of *C. anthurii* (18–20 × 4–4.5 µm) (Delacroix 1897). The combined evidence from phylogenetic analyses, morphological differences, and the absence of significant recombination in PHI test supports the recognition of *C. anthuriicola* as a novel species within the *C. boninense* species complex.

3.4.2 | *Colletotrichum araceiphilum* sp. nov. C. M. Pereira & R. W. Barreto Figure 6

MycoBank: 861823.

Etymology: Based on its seemingly broad host-range within the Araceae.

Typus: Brazil, Minas Gerais, Viçosa, on leaves of *Aglaonema commutatum* (Araceae), 20 July 2022, Robert W. Barreto (RWB 2400), holotype VIC 49392; ex-type living culture COAD 3514.

Description: *sexual morph* not observed. *Hyphae* hyaline to pale brown, smooth, septate, branched, 1.5–5 µm diam. *Conidiomata* acervular, scattered or in groups, black. *Setae* not observed. *Conidiophores* formed in clusters, hyaline to pale brown, smooth, cylindrical, septate, occasionally branched, 12–41.5 × 2.5–6 µm ($\bar{x}$ = 23.5 ± 6.6 × 3.8 ± 0.9 µm), L/W ratio = 6.2. *Conidiogenous cells* formed directly from the mycelium, hyaline, smooth, cylindrical to ampulliform, straight, often curved, 10–33 × 2–5 µm ($\bar{x}$ = 20.3

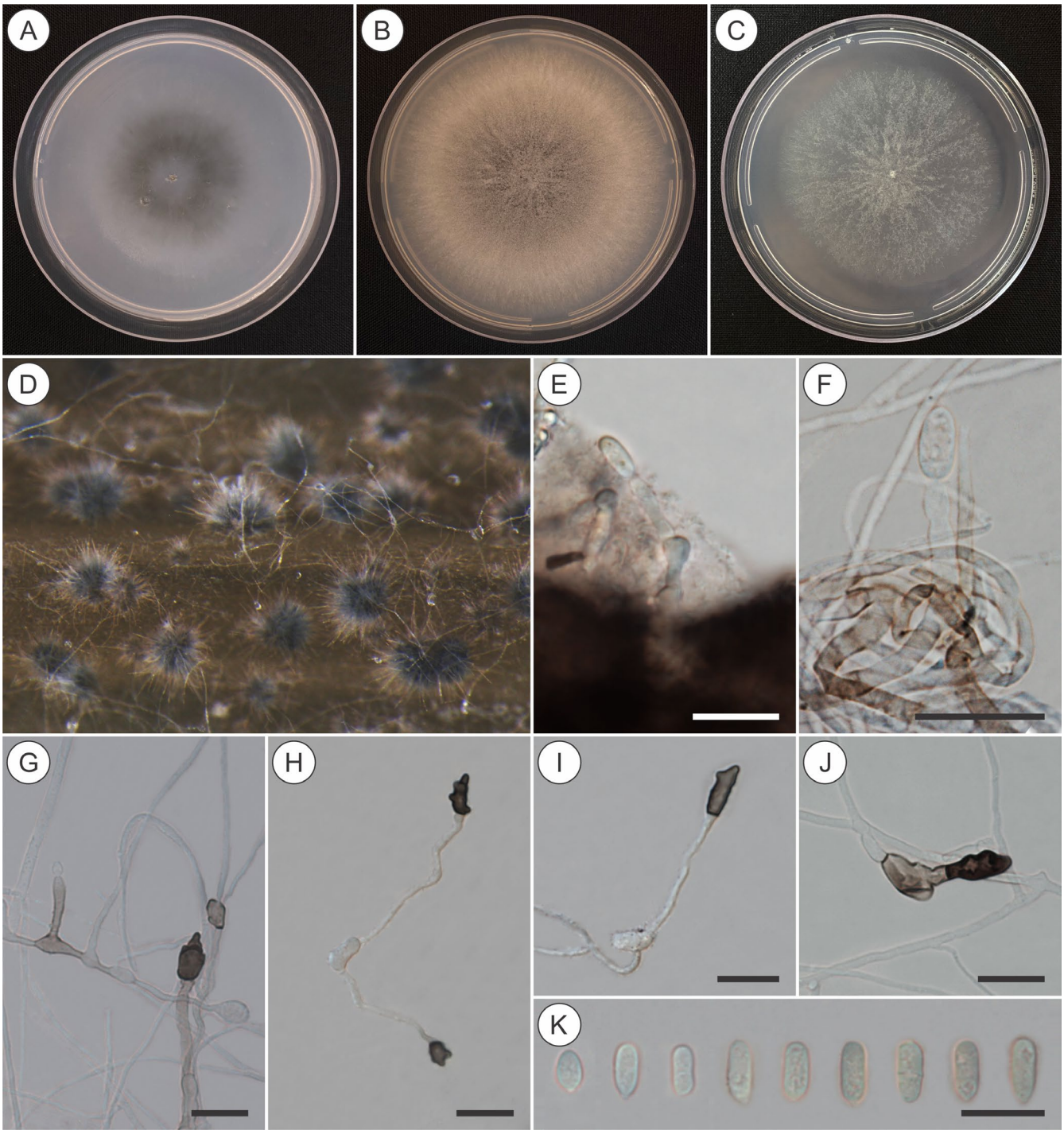


FIGURE 5 | *Colletotrichum anthuriicola* sp. nov. (COAD 3511) from *Anthurium andraeanum*. Colonies on (A) oatmeal agar, (B) potato dextrose agar, and (C) synthetic nutrient-poor agar after 7 days, in the dark at 25°C. (D) Conidiomata formed in vitro on *Petroselinum crispum* stem. (E–G) Conidiophores. (H–J) Appressoria. (K) Conidia. Scale bars—E–K: 20 μm.

± 5.7 × 3.3 ± 0.8 μm), L/W ratio = 6.2. *Conidia* in pale brown masses, hyaline, aseptate, smooth, cylindrical, sometimes obovoid, mostly straight, sometimes slightly curved, with both ends rounded, sometimes rounded at apex but tapering towards a subacute base slightly pointed, hilum indistinct, 11–18 × 4.5–6.5 μm ($\bar{x}$ = 13.3 ± 1.7 × 5.8 ± 0.4 μm), L/W ratio = 2.3. *Appressoria* solitary or in groups, dark brown, smooth, clavate or irregular with entire to undulate margins, 7–21 × 5–14.5 μm ($\bar{x}$ = 12.7 ± 2.7 × 8.7 ± 2.1 μm), L/W ratio = 1.5.

Culture characteristic: colonies on OA fast-growing, 63 mm diam. after 7 days, flat, edge slightly undulate, aerial mycelium feathery with some tufts, olivaceous buff centrally surrounded by white margins; reverse as for the surface. On PDA 62 mm diam. after 7 days, low convex, edge erose, central aerial mycelium cottony, buff, surrounded by area with a few felty patches smoke grey, white margin; reverse as for the surface. On SNA moderate growth, 45 mm diam. after 7 days, low convex, edge undulate, aerial mycelium feathery with some

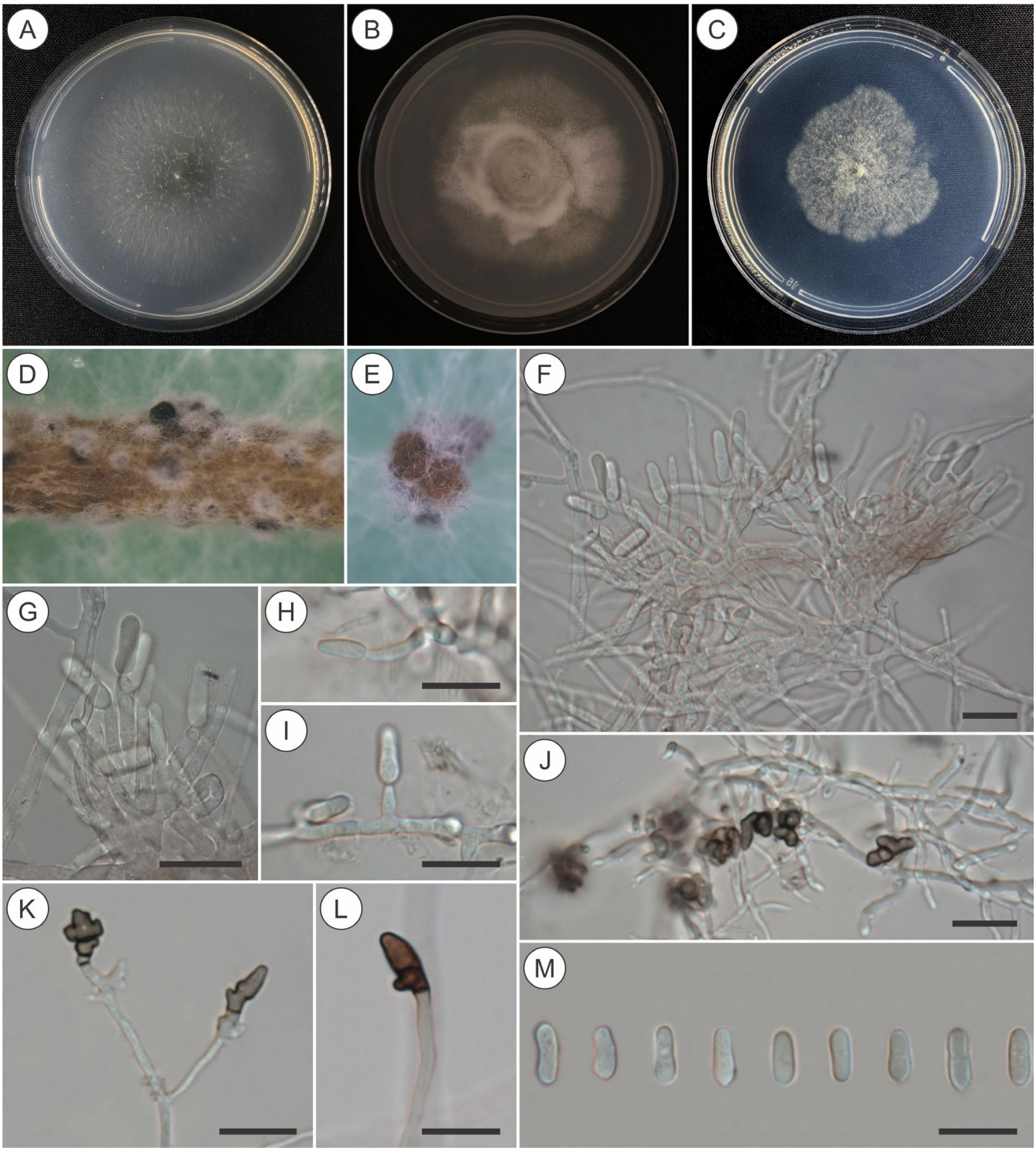


FIGURE 6 | *Colletotrichum araceiphilum* sp. nov. (COAD 3514) from *Aglaonema commutatum*. Colonies on (A) oatmeal agar, (B) potato dextrose agar, and (C) synthetic nutrient-poor agar after 7 days, in the dark at 25°C. (D, E) Conidiomata formed in vitro on *Petroselinum crispum* stem. (F–I) Conidiophores. (J–L) Appressoria. (M) Conidia. Scale bars—F–M: 20 μm.

mycelial tufts, surface and reverse white. Sporulation absent on all media.

Additional material examined: Brazil, Minas Gerais, Viçosa, on leaves of *Philodendron tripartitum* (Araceae), 20th Jul 2022, Robert W. Barreto (coll. number RWB 2399a), VIC 49391; living culture COAD 3512. Brazil, Minas Gerais, Viçosa, on leaves of *Dieffenbachia amoena* (Araceae), 20th Jul 2022, Robert W. Barreto (coll. number RWB 2401), VIC 49393; living culture COAD 3515.

Notes: *C. araceiphilum* is represented by three isolates that formed a well-supported sister branch (79/1) to *C. pseudoboninense*. Besides being reported from an aroid (*P. tatei*) in

China, C. *pseudoboninense* was also found in association with *Dendrobium kingianum* (Orchidaceae) in Japan (Xue et al. 2020).

The sexual morph of *C. araceiphilum* was not obtained; therefore, comparisons with the structures of *C. pseudoboninense* are not possible. However, *C. araceiphilum* has conidiophores and conidia that are longer (up to 41.5 μm long and up to 18 μm long, respectively) than those formed by *C. pseudoboninense* (up to 30 μm long and up to 16.4 μm long, respectively) (Xue et al. 2020). Additionally, appressoria of *C. araceiphilum* (7–21 × 5–14.5 μm) are larger than those of *C. pseudoboninense* (6.6–11.0 × 4.8–8.4 μm) (Xue et al. 2020). Moreover, the PHI test indicated no significant recombination between *C. araceiphilum* and its closest relatives. Another *Colletotrichum* species, *C. aracearum* (latter synonymised to *C. orchidearum*; Damm et al. 2019), has also been reported from Araceae in China, including *Monstera deliciosa* and *Philodendron selloum* (Hou et al. 2016). In addition to belonging to different species complexes—'*C. aracearum*' belongs to the *C. orchidearum* species complex, whereas *C. araceiphilum* belongs to the *C. boninense* species complex. *Colletotrichum araceiphilum* can also be distinguished from '*C. aracearum*' by its shorter conidiophores (up to 41.5 μm long, compared with up to 52 μm long in '*C. aracearum*'), and by its longer conidiogenous cells and appressoria (up to 33 μm and 21 μm long in *C. araceiphilum* versus up to 18 μm and 12.5 μm, respectively, in '*C. aracearum*') (Hou et al. 2016).

3.4.3 | *Colletotrichum imbeicola* sp. nov. C. M. Pereira & R. W. Barreto Figure 7

MycoBank: 861824.

Etymology: Based on the original host name *Philodendron imbe*.

Typus: Brazil, Rio de Janeiro, Rio de Janeiro, Gávea, on leaves of *Philodendron imbe* (Araceae), 4th Jul 2022, Robert W. Barreto (coll. number RWB 2396), holotype VIC 49388; ex-type living culture COAD 3509.

Description: *sexual morph* not observed. *Hyphae* hyaline, smooth, septate, branched, 1–5.5 μm diam. *Conidiomata* acervular, scattered or in groups, black. *Setae* not observed. *Conidiophores* formed in dense clusters, hyaline to pale brown, smooth, cylindrical, septate, occasionally branched, 5–27.5 × 2–4 μm ($\bar{x}$ = 13.9 ± 7.2 × 3.1 ± 0.5 μm), L/W ratio = 4.4. *Conidiogenous cells* formed directly from mycelium, hyaline, smooth, cylindrical to ampulliform, 8–29.5 × 2–5 μm ($\bar{x}$ = 18.8 ± 6 × 3.2 ± 0.8 μm), L/W ratio = 5.8. *Conidia* in orange masses, hyaline, aseptate, smooth, cylindrical to clavate, and reniform, straight to rarely slightly curved, with rounded ends, sometimes with a prominent hilum at the base, 11.5–17.5 × 5–7 μm ($\bar{x}$ = 14.7 ± 1.5 × 5.7 ± 0.5 μm), L/W ratio = 2.6. *Appressoria* solitary, medium to dark brown, smooth, ovoid to irregular, with entire to undulate margins, 6.5–12.5 × 5–11 μm ($\bar{x}$ = 8.6 ± 1.4 × 6.5 ± 1.2 μm), L/W ratio = 1.3.

Culture characteristic: colonies on OA fast-growing 69 mm diam. after 7 days, flat with entire edge, aerial mycelium feathery, with small central mycelial tufts, olivaceous with white margins; reverse as for the surface. On PDA fast-growing 75 mm diam. after 7 days, low convex with entire to slightly undulate edge, aerial mycelium felty, pale luteous, with a smoke grey central area and white periphery; reverse olivaceous buff and white. On SNA fast-growing 58 mm diam. after 7 days, flat with slightly undulate edge, aerial mycelium feathery, with some central tufts, a central area in greenish olivaceous, surrounded by a white ring, reverse as the surface. Sporulation sparse on OA, absent on PDA, and moderate on SNA.

Additional material examined: Brazil, Minas Gerais, Viçosa, Universidade Federal de Viçosa, ornamental plant nursery, on leaves of *Philodendron imbe* (Araceae), 16th Jan 2025, coll. Caio M. Pereira (coll. number DOA 2881), VIC49757; living cultures COAD 4218, COAD 4219 and COAD 4220.

Notes: Isolates of *C. imbeicola* formed a distinct and well-supported clade (100/1) within a larger group comprising *C. karsti*, *C. wuxuhaiense*, *C. spicati*, *C. celtidis*, *C. actinidicola* and *C. philodendrifolium*. Additionally, PHI testing detected no significant recombination between *C. imbeicola* and its closely related species.

Colletotrichum imbeicola seems to be host-specific under field conditions, as all four isolates were obtained from *P. imbe* in two different localities in south-eastern Brazil. Among the closely related species, only *C. karsti* recorded on *Alocasia macrorrhiza* in China (He et al. 2014) and *Anthurium* sp. in Thailand (Damm et al. 2012) were found in association with members of the Araceae. *Colletotrichum philodendrifolium* (recently described below) is also related to *C. imbeicola*.

Morphologically, *C. imbeicola* differs from closely related species by its conidiophores, which are hyaline to pale brown and shorter (up to 27.5 μm long). In contrast, species in the same group produce hyaline, longer conidiophores: *C. karsti* (up to 42 μm; Yang et al. 2011), *C. wuxuhaiense* (up to 31 μm), *C. spicati* (up to 61 μm; Zheng et al. 2022) and *C. philodendrifolium* (up to 37 μm; this study). Comparisons with *C. actinidicola* and *C. celtidis* were not possible, as conidiophore measurements were not provided in the original description of *C. actinidicola*, and in *C. celtidis* these structures were reported as reduced conidiogenous cells (Tennakoon et al. 2021; Norphanphoun et al. 2025).

Conidiogenous cells also differ in size, being longer in *C. imbeicola* (up to 29.5 μm in length) than in the other species, including *C. karsti* (up to 20 μm; Yang et al. 2011), *C. wuxuhaiense* (up to 15.8 μm; Zheng et al. 2022), *C. celtidis* (up to 16 μm; Tennakoon et al. 2021), *C. spicati* (up to 2.6 μm; Zheng et al. 2022) and *C. philodendrifolium* (up to 27 μm; noted in this publication). However, they are shorter than those of *C. actinidicola* (up to 40 μm; Norphanphoun et al. 2025). In addition, conidia of *C. imbeicola* produce some reniform and cylindrical to clavate conidia. Conidia are always straight in *C. karsti* (Yang et al. 2011). *C. wuxuhaiense* has oval conidia (Zheng et al. 2022). *C. spicati* has ellipsoidal to subglobose, sometimes cylindrical, conidia (Zheng et al. 2022). *C. celtidis* has ellipsoidal to ovoid, rarely clavate to cylindrical, conidia (Tennakoon et al. 2021). *C. actinidicola* has ellipsoidal to cylindrical conidia (Norphanphoun et al. 2025), and

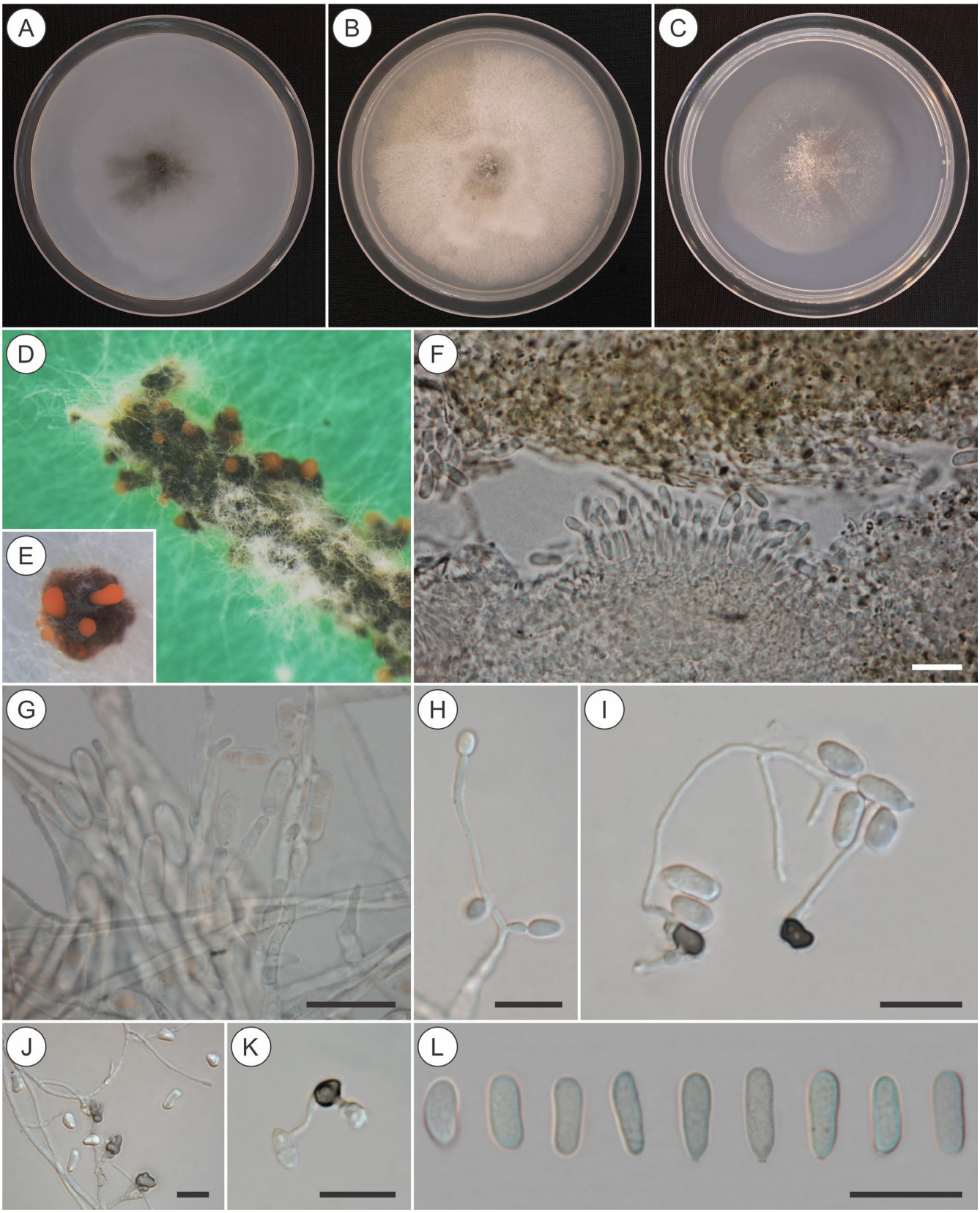


FIGURE 7 | *Colletotrichum imbeicola* sp. nov. (COAD 3509) from *Philodendron imbe*. Colonies on (A) oatmeal agar, (B) potato dextrose agar, and (C) synthetic nutrient-poor agar after 7 days, in the dark at 25°C. (D, E) Conidiomata formed in vitro on *Petroselinum crispum* stem. (F–H) Conidiophores. (I–K) Appressoria. (L) Conidia. Scale bars—F–L: 20 μm.

C. philodendrifolium produces cylindrical, but also pyriform to clavate conidia (noted in this publication).

3.4.4 | *Colletotrichum philodendrifolium* sp. nov. C. M. Pereira & R. W. Barreto Figure 8

MycoBank: 861825.

Etymology: Based on the name of its original host-genus.

Typus: Brazil, Minas Gerais, Viçosa, on leaves of *Philodendron tripartitum*, (Araceae), 20th Jul 2022, Robert W. Barreto (coll. number RWB 2399c), holotype VIC 49391; ex-type living culture COAD 3513.

Description: *sexual morph*: formed after 15 days on SNA. *Ascomata* globose to ellipsoidal sometimes pyriform, solitary or in small groups, black, superficial or immersed on SNA, 74–268 × 68–182 μm ($\bar{x}$ = 141.7 ± 54.1 × 124.9 ± 39.2 μm), L/W ratio = 1.1. *Asci* cylindrical to clavate, hyaline, 30–60.5 × 5–11 μm, ($\bar{x}$ = 46.7 ± 9.8 × 8.2 ± 1.5 μm), L/W ratio = 5.7, 8 spored. *Ascospores* uni- or biseriate, hyaline, smooth, aseptate, allantoid to somewhat fusiform with rounded-ends, 12–20 × 3.5–5.5 μm ($\bar{x}$ = 15.2 ± 1.7 × 4.2 ± 0.5 μm), L/W ratio = 3.6. *Hyphae* hyaline, smooth, septate, branched, 1–5 μm diam. *Conidiomata* acervular, scattered or in groups, black. *Setae* not observed. *Conidiophores* formed in clusters, hyaline, smooth, cylindrical, septate, occasionally branched, 8–37 × 2–5.5 μm ($\bar{x}$ = 15.7 ± 6.5 × 3.7 ± 0.7 μm), L/W ratio = 4.2. *Conidiogenous cells* hyaline, smooth, cylindrical to ampulliform, 6.5–27 × 2.5–4.5 μm ($\bar{x}$ = 15.3 ± 4.7 × 3.4 ± 0.6 μm), L/W ratio = 4.4. *Conidia* hyaline, aseptate, smooth, cylindrical, pyriform to clavate, mostly straight, sometimes curved, rounded at both ends, with no visible scar at base, 9–17.5 × 4.5–6.5 μm ($\bar{x}$ = 12.3 ± 1.9 × 5.4 ± 0.5 μm), L/W ratio = 2.3. *Appressoria* solitary, medium to dark brown, smooth, mostly ovoid, but sometimes irregular in shape, with entire to undulate margins, 7.5–13 × 4.5–9 μm ($\bar{x}$ = 9.4 ± 1.3 × 6.7 ± 1.1 μm), L/W ratio = 1.4.

Culture characteristic: colonies on OA fast-growing 58 mm diam. after 7 days, flat with slightly undulate edge, aerial mycelium felty, with patches of orange conidial masses, salmon to apricot centrally, surrounded by white periphery; reverse salmon with white margin. On PDA 56 mm diam. after 7 days, low convex with entire edge, aerial mycelium felty, fuscous black, surrounded by rosy buff area and white margins; reverse as for the surface. On SNA 56 mm diam. after 7 days, flat with entire edge, aerial mycelium feathery to felty with some central black tufts, surface and reverse white. Sporulation abundant on OA, scarce on PDA, and absent on SNA.

Notes: *C. philodendrifolium* is represented by a single isolate, that formed a distinct branch (48/0.99) relative to *C. actinidicola*, *C. spicati* and *C. celtidis*. The sexual morph was observed in COAD 3513 but not in any other isolate obtained during our sampling. Sexual morphs of *C. actinidicola*, *C. celtidis* and *C. spicati* were also not reported in the original descriptions of those species (Tennakoon et al. 2021; Zheng et al. 2022; Norphanphoun et al. 2025). Nevertheless, Zhang, Nizamani, et al. (2023) described the sexual morph for *C. celtidis* later. The comparison of *C. philodendrifolium* with the morphology provided in Zhang's description of *C. celtidis* and *C. spicati* highlighted some relevant morphological differences. *C. philodendrifolium* has smaller asci (30–60.5 × 5–11 μm) and ascospores (12–20 × 3.5–5.5 μm) than those of *C. celtidis* (asci: 40.5–78 × 8.2–20 μm; ascospores: 16.5–25 × 4.5–8 μm) (Zhang, Nizamani, et al. 2023).

There are also morphological differences for the asexual morph. Conidiophores of *C. philodendrifolium* are shorter than those of *C. spicati* (up to 37 μm vs. up to 61 μm, respectively) (Zheng et al. 2022). In addition, *C. philodendrifolium* has longer conidiogenous cells (up to 27 μm) than *C. spicati* (up to 2.6 μm) (Zheng et al. 2022) and *C. celtidis* (up to 16 μm) (Tennakoon et al. 2021), but shorter than those of *C. actinidicola* (up to 40 μm) (Norphanphoun et al. 2025).

The new species *C. philodendrifolium* was obtained from *P. tripartitum* in Brazil, whereas *C. actinidicola*, *C. celtidis* and *C. spicati* appear to be restricted to China, in association with plants across various families. *C. actinidicola* was found on symptomatic leaves of *Actinidia chinensis* (Actinidiaceae) (Norphanphoun et al. 2025). *C. celtidis* was originally found occurring as a saprobe on dead leaves of *Celtis formosana* (Cannabaceae). More recent reports describe it in association with *Rhododendron simsii* (Ericaceae), *Magnolia denudata* (Magnoliaceae) (Zhang, Nizamani, et al. 2023), and as the causal agent of leaf anthracnose on plum (*Prunus salicina*, Rosaceae) (Wang et al. 2024). Isolates of *C. spicati* were obtained as endophytes from the stem of *Myriophyllum spicatum* (Haloragaceae) and from the roots of *Potamogeton wrightii* (Potamogetonaceae) (Zheng et al. 2022), both of which are aquatic and/or semi-aquatic plants.

Additionally, the PHI test showed no significant evidence of recombination between *C. philodendrifolium* and its closely related species. Thus, the combined evidence from phylogenetic analyses, morphological differences and the absence of recombination supports the recognition of this taxon as a novel species within the *C. boninense* species complex.

3.5 | Pathogenicity Tests

All isolates included in our inoculation studies (COAD 3509, COAD 3511, COAD 3513 and COAD 3514) were pathogenic to at least three of the inoculated aroids (Table 1). *Anthurium andraeanum* was the only host that remained symptomless after being inoculated with each of the isolates, including the new species *C. anthuriicola* isolated from anthurium and first described in this study. This result contrasts with those obtained for the other test plants and was consistent regardless of the inoculation method (wounded or unwounded) or inoculum type (mycelial discs or conidial suspensions). Control unwounded plants treated with non-colonised PDA medium or sprayed with tap water remained healthy. Wounded control plants that received tap water or PDA discs developed necrotic injuries only at the damaged areas (Figures 9A,J and 10A,F,J). No *Colletotrichum* colonies were obtained from necrotic tissues at the injured points of control plants.

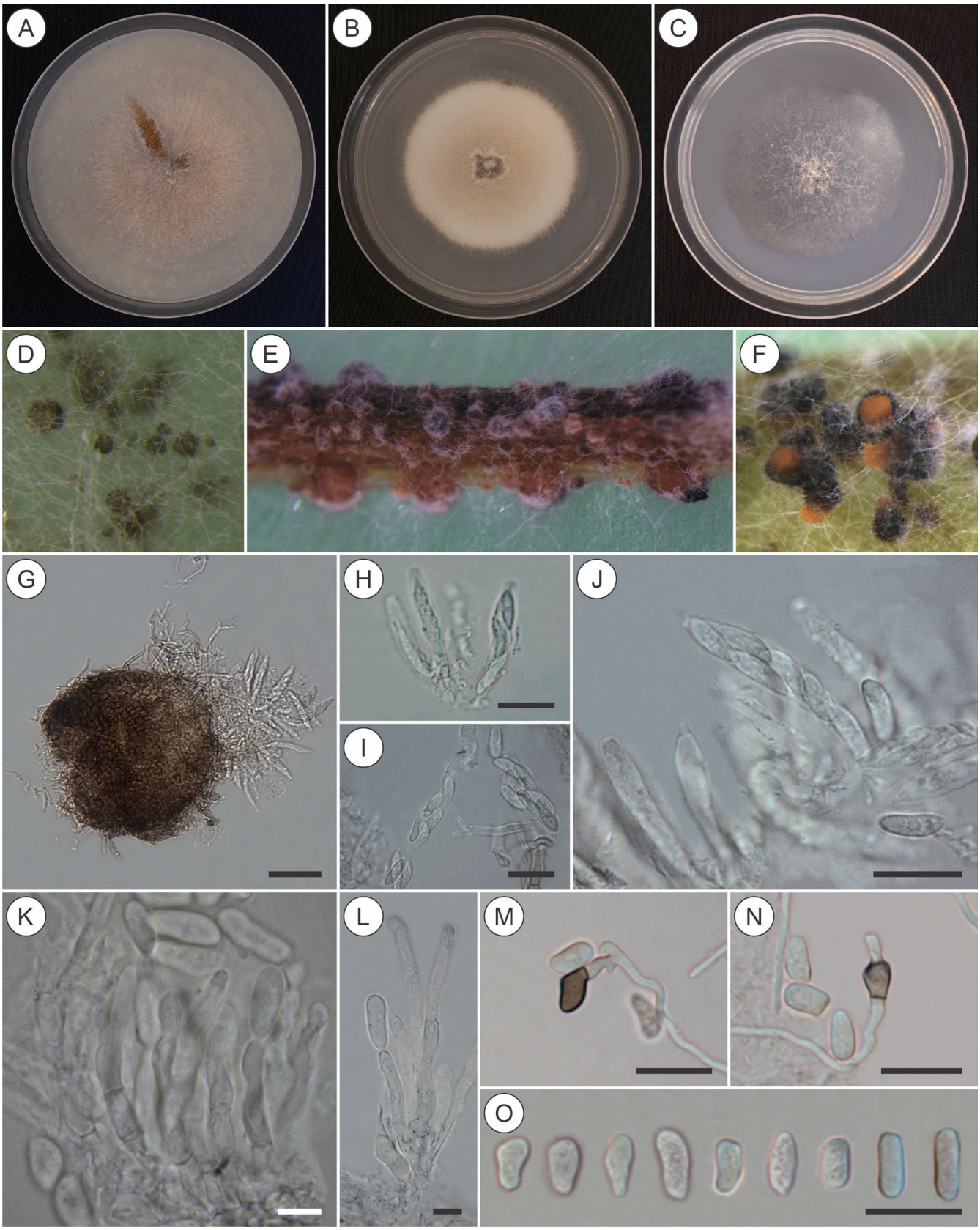


FIGURE 8 | *Colletotrichum philodendrifolium* sp. nov. (COAD 3513) from *Philodendron tripartitum*. Colonies on (A) oatmeal agar, (B) potato dextrose agar, and (C) synthetic nutrient-poor agar after 7 days, in the dark at 25°C. (D) Ascomata on synthetic nutrient-poor agar. (E, F) Conidiomata formed in vitro on *Petroselinum crispum* stem. (G) Ascomata. (H–J) Asci and ascospores. (K–L) Conidiophores. (M–N) Appressoria. (O) Conidia. Scale bars—G: 50 μm; H–O: 20 μm.

TABLE 1 | Cross-inoculations of *Colletotrichum* spp. isolates obtained from ornamental Araceae in Brazil onto selected ornamental aroids.

Fungal species (isolate)	Inoculum[a,b]	Test plant[c,d]											
		Anthurium andraeanum		*Aglaonema commutatum*		*Dieffenbachia amoena*		*Epipremnum aureum*		*Philodendron imbe*		*Philodendron tripartitum*	
		Intact	Wounded	Intact	Wounded	Intact	Wounded	Intact	Wounded	Intact	Wounded	Intact	Wounded
Colletotrichum imbeicola (COAD 3509)	Susp.	–	W	+	+	–	+	–	+	–	W	–	W
	Disc	–	W	+	+	+	+	–	+	+[§]	+	–	W
Colletotrichum anthuriicola (COAD 3511)	Susp.	–	W	–	+	–	+	–	+	–	W	–	W
	Disc	–	W	+	+	+	+	–	+	–	W	–	W
Colletotrichum philodendrifolium (COAD 3513)	Susp.	–	W	–	+	–	+	–	W	–	W	–	W
	Disc	–	W	–	W	–	+	–	+	–	W	–	+
Colletotrichum araceiphilum (COAD 3514)	Susp.	–	W	+	+	–	+	–	+	–	W	–	W
	Disc	–	W	+	+	+	+	–	+	–	+	–	W
Control	SDW	–	W	–	W	–	W	–	W	–	W	–	W
	PDA	–	W	–	W	–	W	–	W	–	W	–	W

[a]Susp.: suspension of conidia; Disc: mycelial discs.
[b]Control: SDW, sterile distilled water; PDA, uncolonised discs of potato dextrose agar.
[c]Intact: not damaged plants; wounded: plants wounded at the inoculation spots with a sterile needle incursion.
[d]–: no symptoms; W: wounding symptoms; +: disease symptoms; +[§]: leaf spots observed but without successful reisolation.

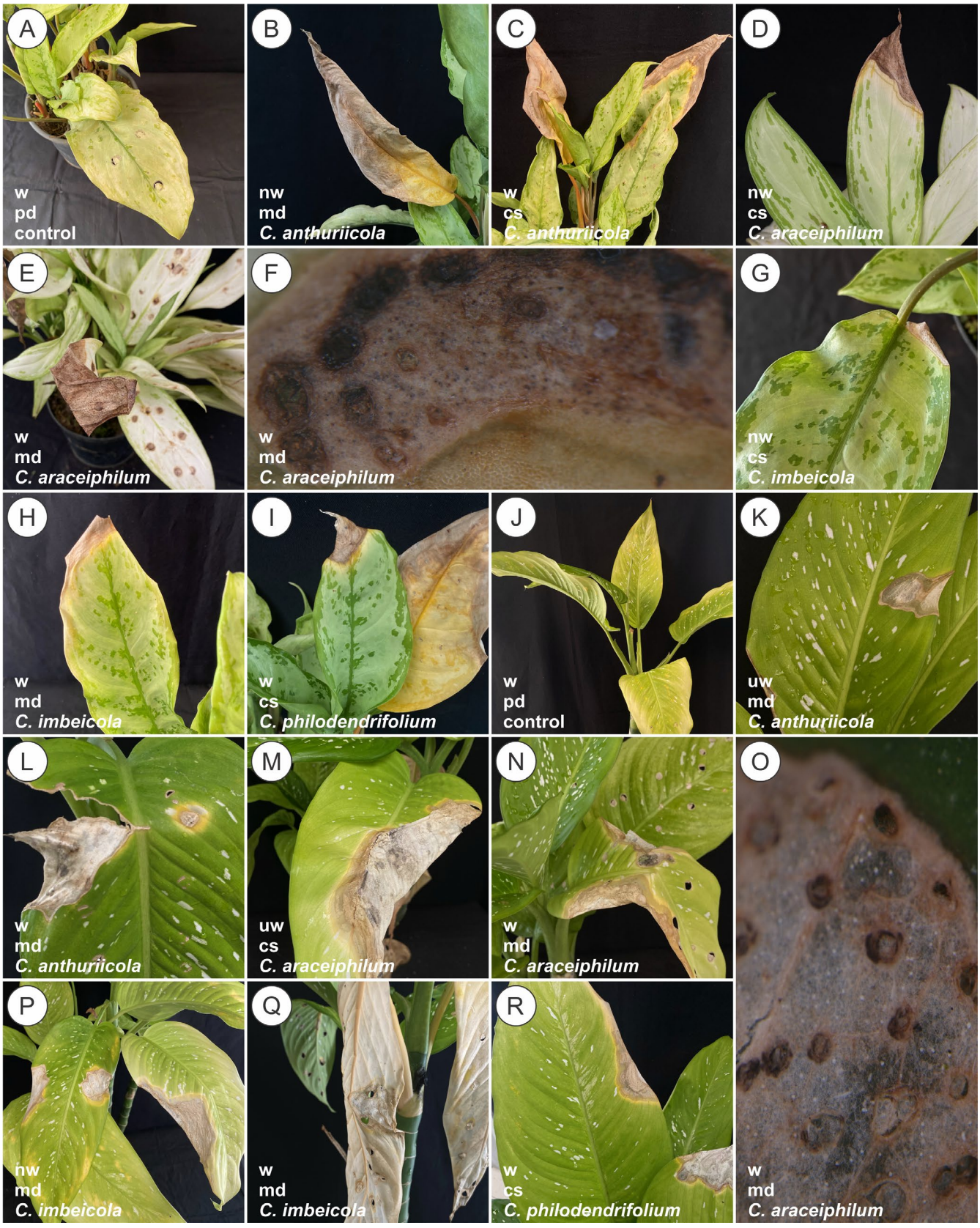


FIGURE 9 | Results of pathogenicity tests of *Colletotrichum* species on aroids. (A–I) *Aglaonema commutatum* and (J–R) *Dieffenbachia amoena* plants, either unwounded (uw) or wounded (w), treated with potato dextrose agar discs (pd, control), or with conidial suspension (cs) or mycelial discs (md) of *Colletotrichum anthuriicola* (COAD 3511), *C. araceiphilum* (COAD 3514), *C. imbeicola* (COAD 3509) and *C. philodendrifolium* (COAD 3513).

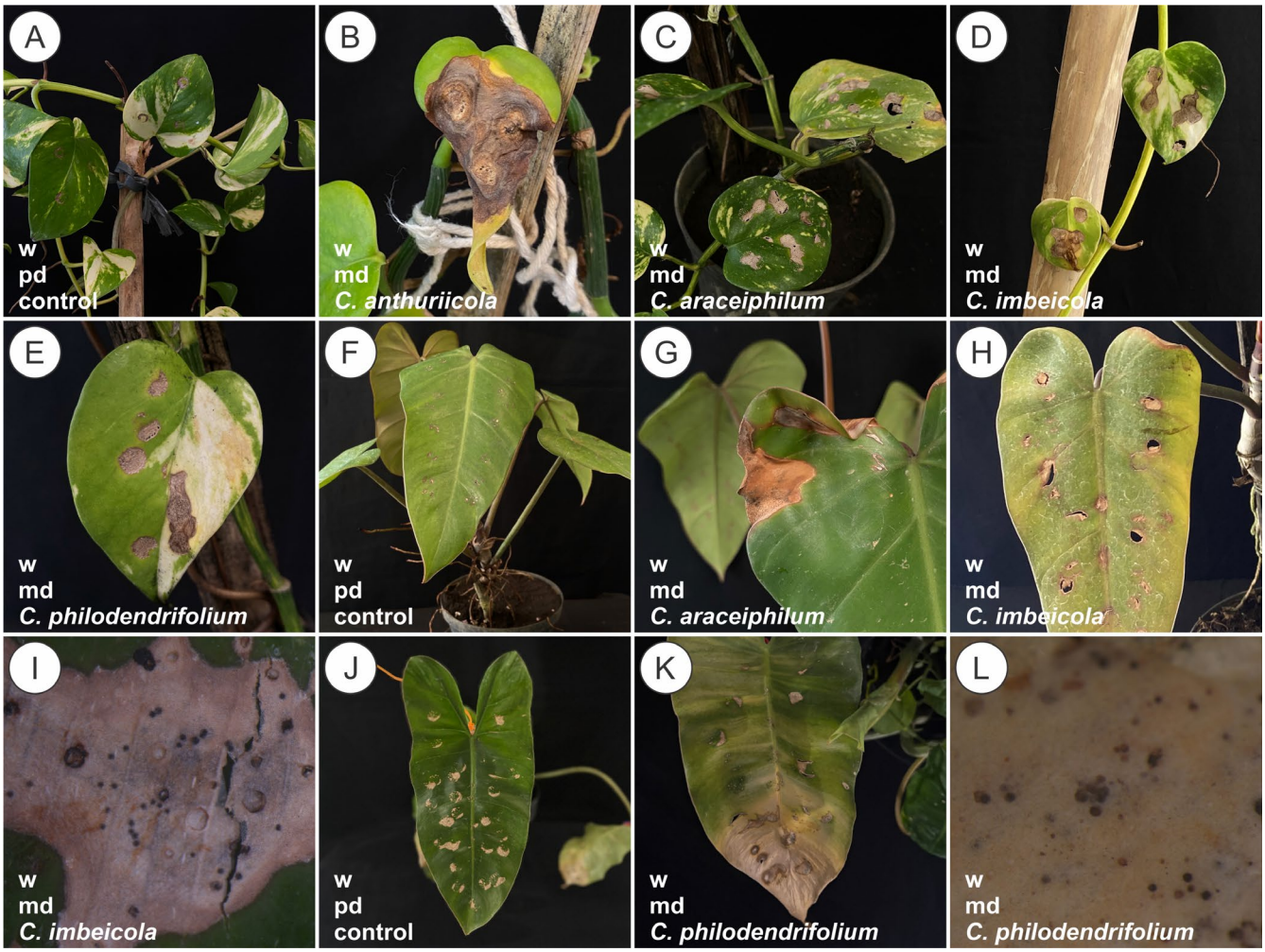


FIGURE 10 | Results of pathogenicity tests of *Colletotrichum* species on aroids. (A–E) *Epipremnum aureum*, (F–I) *Philodendron imbe*, and (J–L) *Philodendron tripartitum* plants, wounded (w), treated with potato dextrose agar discs (pd, control), or with mycelial discs (md) of *Colletotrichum anthuriicola* (COAD 3511), *C. araceiphilum* (COAD 3514), *C. imbeicola* (COAD 3509) and *C. philodendrifolium* (COAD 3513).

Aglaonema commutatum (Figure 9B–I), *D. amoena* (Figure 9K–O) and *E. aureum* (Figure 10B–E) were susceptible to all *Colletotrichum* isolates included in the test. Symptoms appeared 21 days after inoculation (DAI). In most cases, wounding led to a higher frequency of anthracnose symptoms. The isolates were successfully reisolated from such symptomatic tissues 28 DAI and colonies with the typical morphology for each species were obtained, thereby fulfilling Koch's postulates for isolate COAD 3514, originally obtained from *A. commutatum*.

Philodendron imbe was susceptible to two isolates, COAD 3514 (Figure 10G) and COAD 3509 (Figure 10H,I). Nevertheless, symptoms only developed on plants inoculated with mycelial discs 21 DAI. Both isolates were reisolated from wounded and symptomatic plants 28 DAI, fulfilling Koch's postulates for COAD 3509. Although symptoms were also observed on one unwounded plant, inoculated with COAD 3509, unexpectedly, the fungus could not be reisolated from the diseased tissue of its own original host. This result remains unclear. Anthracnose symptoms on *Philodendron tripartitum* were observed only on wounded plants inoculated with *C. philodendrifolium* (COAD 3513), and only when mycelial discs were used as the inoculum source (Figure 10K,L). Symptoms appeared 21 DAI, and reisolations from tissues collected 28 DAI exhibited the typical morphology of *C. philodendrifolium*, therefore fulfilling Koch's postulates for this species.

4 | Discussion

Although the ITS region has been proposed as a universal DNA fungal barcode marker (Schoch et al. 2012), it has limited utility for systematic studies of *Colletotrichum* (Vieira et al. 2020) and several additional markers are needed. According to Damm et al. (2012), Vieira et al. (2020) and Bhunjun et al. (2021), fragments of *gapdh*, *his3* and *tub2* are appropriate for initial diversity screening across most species' complexes. Given this, these regions were sequenced as a first step and showed that all isolates examined belong to the *C. boninense* species complex (Figure S1). To obtain better resolution and evaluate species boundaries with respect to our isolates, four other genetic markers were sequenced and included in the multigene analyses (i.e., *act*, *cal*, *chs-1* and ITS), as per others who have examined this complex (e.g., Liu et al. 2022; Vieira et al. 2020; Xue et al. 2020; Zapata et al. 2024; Zhang, Chen, et al. 2023). Individual gene phylogenies were obtained and variable resolution among loci

was observed (Figure S2). The *gapdh* and *his3* regions resolved multiple species, while *act*, *cal* and *tub2* regions resolved some of the proposed taxa with moderate support. These results showed that individual loci contribute partially to species delimitation, and that the partial sequences of *his3*, *cal* and *gapdh* improved the resolution of the combined tree.

Although *his3* and *gapdh* regions were not available for some species within the *C. boninense* species complex, our results indicated that these loci may be useful for species delimitation in this group. The phylogenetic topology obtained from the analysis excluding these regions (Figure S3) was consistent with that inferred from the seven-locus dataset.

Species delimitation within *Colletotrichum* is continuously being revised. More recently, Zhang, Nizamani, et al. (2023) synonymised *C. wuxuhaiense* with *C. karsti* based on morphological similarities and analyses of a concatenated dataset comprising six genetic regions (ITS, *gapdh*, *chs-1*, *his3*, *act* and *tub2*). However, in the original description, Zheng et al. (2022) reported that *C. wuxuhaiense* produces shorter conidia (10.3–15.8 μm × 4.7–8.9 μm) compared to *C. karsti* (12.5–19.5 μm × 6.0–8.5 μm), and those two isolates formed a distinct clade from *C. karsti*. Although no representatives of *C. wuxuhaiense* were obtained in this study, our phylogenetic analyses—based on the same six loci used by Zhang, Nizamani, et al. (2023), with the addition of the *cal* region—are consistent with the findings of Zheng et al. (2022), as isolates of *C. wuxuhaiense* formed a distinct and well-supported clade (99/1) relative to *C. karsti*. Therefore, re-examining and obtaining new isolates of *C. wuxuhaiense* would be necessary to clarify this issue.

Traditionally (with the exception of crops such as roses, chrysanthemums, orchids, turfgrasses and a few other groups), ornamental plants have received limited attention from plant pathologists. More recently, however, studies on ornamental plant diseases—particularly anthracnoses and their aetiological agents—have gained increasing attention (Guarnaccia et al. 2021; Talhinhas and Baroncelli 2023; Zhang, Chen, et al. 2023).

For example, *Colletotrichum* species have been isolated and identified both as endophytes (Ma et al. 2018; Tao et al. 2013) and pathogens (Silva et al. 2021; Silva-Cabral et al. 2019; Yang et al. 2011) on Orchidaceae, whereas *C. truncatum* and *C. karsti* have been recognised as the causal agents of stem and leaf lesions on *Begonia* spp. (Begoniaceae) (Wu et al. 2022; Zhai et al. 2018).

There are reports of *C. capsici* and *C. gloeosporioides* associated with *A. commutatum* in Venezuela and India (Farr et al. 2026). On *A. andraeanum*, in addition to *C. gloeosporioides*, *C. fructicola*, *C. orchidearum* and *C. siamense* have been reported to cause spathe rot, spadix rot and leaf spots in Sri Lanka (Vithanage et al. 2021). In Brazil, *C. theobromicola* has been associated with anthracnose on *Anthurium* flowers (Chaves et al. 2020), whereas *C. karsti* has been isolated from *Anthurium* sp. in Thailand (Damm et al. 2019).

There are three records of *C. gloeosporioides* on *D. amoena* in Iran and the United States; however, these are old records (Farr et al. 2026) that do not include molecular-based identification or indicate reference material deposited in fungaria, nor pure cultures deposited in public culture collections. For *Philodendron*, 36 records of *Colletotrichum* are available, including the species *C. aracearum*, *C. gloeosporioides*, *C. lindemuthianum*, *C. orchidearum*, *C. philodendri*, *C. pseudoboninense* and *C. siamense* (Farr et al. 2026), none of which are reported in Brazil.

Although no *Colletotrichum* isolates were obtained from *E. aureum* and *S. podophyllum*, there are published records of *Colletotrichum* spp. associated with these hosts. *C. gloeosporioides* has been reported on *E. aureum* in Brazil (Mariano et al. 1989; Paz et al. 1998), whereas *C. orchidearum* has been reported on this host in Iran (Damm et al. 2019). For *S. podophyllum*, two records of *C. gloeosporioides* were also published, from the United States and China (Farr et al. 2026). Nevertheless, early records of *C. gloeosporioides* must be regarded as doubtful because these were published in the 'pre-molecular' age, and, at that time of publication, *C. gloeosporioides* was used as a collective name for anthracnose fungi.

Our inoculation results indicated that *A. commutatum* and *D. amoena* are susceptible to various species of *Colletotrichum*. All isolates involved in the study were able to infect and cause symptoms on their leaves, both on unwounded and wounded plants. *E. aureum* was also susceptible to all isolates; however, only wounded leaves became infected. This reaction has been previously observed in our earlier study involving leaf spots on golden pothos. In that instance, *Cercospora* isolates could cause disease only on wounded *E. aureum* leaves (Pereira et al. 2024), suggesting that *Cercospora*, and now also *Colletotrichum*, require wounds to infect the tissues of this host. This also implies that this aroid species possesses some level of resistance conferred by physical and/or chemical barriers at the epidermis level. Similar indications were obtained from inoculations of *P. imbe* and *P. tripartitum*, as *Colletotrichum* isolates were only capable of causing anthracnose symptoms on wounded plants.

Under experimental conditions, leaves of *A. andraeanum* remained healthy regardless of inoculation methods or the type of inoculum used. Based on this, we hypothesise that specific predisposing factors may be required for the development of anthracnose on *A. andraeanum*, particularly sun scorch damage preceding infection by *Colletotrichum* spp. There was an earlier indication from a study by our research group, involving inoculations of *Colletotrichum* isolates obtained from anthracnose on anthurium (unpublished data), which failed to reproduce the striking blight symptoms observed in the field. This assumption was based on repeated field observations of anthracnose occurring on anthurium plants that were growing directly exposed to the sun, whereas nearby plants growing in the shade had little to no disease symptoms. These observations have been made at several locations and possibly mirror the adaptation of anthurium to its original habitat in the understorey of the forests in the upper Amazon (Liu et al. 2024). Additional experiments under controlled conditions may fully clarify this hypothesis in the future. A similar contrast between sun-exposed and shaded plants, with severe anthracnose developing only under full sun exposure, was also observed for *P. imbe* at the type locality of *C. imbeicola* during our observations in Rio de Janeiro. The connection between anthracnose intensity and sun exposure (or high light

intensity) has been documented for other crops, including avocado (*Persea americana*), the ornamental plant *Euonymus fortune*, hot pepper (*Capsicum annuum*), strawberry (*Fragaria* × *ananassa*) and tea (*Camellia sinensis*) (Gao et al. 2021; Ningen et al. 2005; Smith et al. 2023; Tinyane et al. 2018; Ye et al. 2024). Depending on the rate and exposure time, ultraviolet radiation (UV-A, -B and -C) can have positive effects on disease resistance (Mmbando 2023), but may also induce stresses, leading to severe damage to DNA, proteins, other cellular components and tissues (Müller-Xing et al. 2014; Vanhaelewyn et al. 2020), thereby creating potential entry points for pathogens. This hypothesis remains to be tested, particularly in the case of *A. andraeanum* and *Philodendron* spp. The possibilities of the *Colletotrichum* spp. described here to function as either saprophytes or endophytes, in association with their original hosts and other aroids, should also be investigated. Our inoculation studies indicate that *Colletotrichum* spp. associated with Araceae are mostly polyphagous within the family and capable of colonising and causing disease in a range of different genera. This pattern appears to be common for the genus, as exemplified by *C. orchidearum* (as *C. aracearum*) attacking *Monstera deliciosa* and *Philodendron selloum* in China (Hou et al. 2016), and *C. siamense* causing leaf spots on *Alocasia macrorrhiza*, *M. deliciosa*, *Philodendron bipinnatifidum* in China (Huang et al. 2021; Liu et al. 2021; Ning et al. 2022), as well as on *Amorphophallus paeoniifolius* in India (Prasad et al. 2017). Additionally, the isolation of more than one *Colletotrichum* species from a single Araceae host suggests that this is common for anthracnose fungi on aroids, as in the case of *C. siamense* and *C. tropicale* causing anthracnose of *Syngonium podophyllum* in China (Cui et al. 2025), and *C. brevisporum* and *C. musicola* causing leaf anthracnose of *Colocasia esculenta* in Mexico (Vásquez-López et al. 2019).

This information is particularly relevant for the management of anthracnose on aroids because neighbouring members of the Araceae in commercial plantations (even if belonging to distantly related species) may serve as inoculum reservoirs for infection of healthy plants. Moreover, our results highlight that defences at the epidermal level may be of great importance against aroid anthracnose and protection, be artificially induced injuries often allowed the disease to establish. Thus, protection against plant tissue injury (particularly sun scorch) may be critical for avoiding problems with aroid anthracnose.

Many ornamental plants are affected by *Colletotrichum* (Guarnaccia et al. 2021; Zhang, Chen, et al. 2023), and in the family Araceae *Colletotrichum* spp. have been reported to cause anthracnose on members of *Alocasia*, *Amorphophallus*, *Anthurium*, *Dieffenbachia*, *Epipremnum*, *Monstera*, *Philodendron*, *Rhaphidophora*, *Spathiphyllum*, *Syngonium*, among others (Talhinhas and Baroncelli 2023). In Brazil, *Colletotrichum* spp. have been reported only on the following aroids genera: *Anthurium*, *Dieffenbachia*, *Epipremnum* and *Heteropsis* (Farr et al. 2026). However, most of the records listed in the latter are only from disease indexes (EMBRAPA 2026; Farr et al. 2026) and are therefore incomplete, often identifying the anthracnose agent only as *Colletotrichum* sp., or are outdated from a taxonomic perspective, referring to the pathogen as '*Colletotrichum gloeosporioides*'. Furthermore, many of these records are unsupported by reference fungarium specimens or pure cultures deposited in public culture collections. Future studies, including those focused on disease management, should include a more precise taxonomic elucidation of the fungi involved in the anthracnose of ornamental aroids.

There are no contemporary studies focusing on *Colletotrichum* spp. on Araceae in Brazil, including the use of molecular tools for species identification. The potential for expanding the knowledge of the mycodiversity, either on native aroids or introduced cultivated taxa seems to be great, as revealed by our brief survey, limited in time and space. Most of the sampling performed in this present study was conducted on a single day (20 July 2022) at a single location (e.g., the ornamental plant nursery in the campus of the University of Viçosa). Plants representing eight species across seven aroid genera were collected. Of these, five species were found to be infected by *Colletotrichum* spp., yielding only nine fungal isolates. Despite the limited number of isolates, a surprisingly high diversity of *Colletotrichum* was recovered, with four distinct species identified, all of which are recognised here as new to science. This highlights the value of host family-focused surveys for uncovering fungal diversity.

Author Contributions

Caio Mattos Pereira: methodology, investigation, formal analysis, visualization, writing – original draft, data curation. **Robert Weingart Barreto:** conceptualization, writing – review and editing, project administration, supervision, investigation.

Acknowledgements

Caio M. Pereira acknowledges financial support from the Conselho Nacional de Desenvolvimento Científico e Tecnológico (CNPq) (Project 141346/2021-3). The Article Processing Charge for the publication of this research was funded by the Coordenação de Aperfeiçoamento de Pessoal de Nível Superior - Brasil (CAPES) (ROR identifier: 00x0ma614).

Conflicts of Interest

The authors declare no conflicts of interest.

Data Availability Statement

The data that support the findings of this study are available from the corresponding author upon reasonable request. Sequences were deposited in GenBank (accession numbers are in Table S1).

References

Bhunjun, C. S., C. Phukhamsakda, R. S. Jayawardena, R. Jeewon, I. Promputtha, and K. D. Hyde. 2021. "Investigating Species Boundaries in *Colletotrichum*." *Fungal Diversity* 107: 107–127.

Bruen, T. C., H. Philippe, and D. Bryant. 2006. "A Simple and Robust Statistical Test for Detecting the Presence of Recombination." *Genetics* 172: 2665–2681.

Chaudhuri, T., B. Panja, and J. Saha. 2018. "Studies on Cultural, Morphological and Biochemical Aspects of *Colletotrichum acutatum* of *Aglaonema* Using Various Carbon Sources." *International Journal of Current Microbiology and Applied Sciences* 7: 2600–2606.

Chaves, T. P., A. R. G. S. Miranda, L. C. da Paz, M. S. B. Netto, G. S. A. Lima, and I. P. Assunção. 2020. "First Report of *Colletotrichum theobromicola* Causing Anthracnose on *Anthurium* sp." *Australasian Plant Disease Notes* 15: 27.

Corda, A. 1831. "Die Pilze Deutschlands." In *Deutschlands Flora in Abbildungen nach der Natur mit Beschreibungen*, edited by J. Stum, 33–64. Gedruckt auf Kosten des Verfassers/Herausgebers.

Crous, P. W., G. J. M. Verkley, J. Z. Groenewald, and J. Houbraken. 2019. *Fungal Biodiversity*. Westerdijk Fungal Biodiversity Institute.

Cui, J., J. Sun, M. Li, et al. 2025. "First Report of *Colletotrichum siamense* and *C. tropicale* Causing Anthracnose of *Syngonium podophyllum* in China." *Crop Protection* 187: 106978.

Damm, U., P. F. Cannon, J. H. C. Woudenberg, et al. 2012. "The *Colletotrichum boninense* Species Complex." *Studies in Mycology* 73: 1–36.

Damm, U., T. Sato, A. Alizadeh, J. Z. Groenewald, and P. W. Crous. 2019. "The *Colletotrichum dracaenophilum*, *C. magnum* and *C. orchidearum* Species Complexes." *Studies in Mycology* 92: 1–46.

Darriba, D., G. L. Taboada, R. Doallo, and D. Posada. 2012. "jModelTest 2: More Models, New Heuristics and Parallel Computing." *Nature Methods* 9: 772.

Data Bridge Market Research (DBMR). 2025. *Global Flowers and Ornamental Plants Market – Industry Trends and Forecast to 2029*. DBMR.

de Álvarez, M. C., and R. Álvarez. 2001. "First Report of *Colletotrichum dematium* on *Aglaonema* and of *C. gloeosporioides* on *Syngonium* in the Northeast of Argentina." *Investigacion Agraria Produccion y Proteccion Vegetales* 16: 131–134.

Dean, R., J. A. L. Van Kan, Z. A. Pretorius, et al. 2012. "The Top 10 Fungal Pathogens in Molecular Plant Pathology." *Molecular Plant Pathology* 13: 414–430.

Delacroix, M. G. 1897. *Espèces Parasites Nouvelles*. Bulletin de la Société mycologique de France.

EMBRAPA. 2026. *Fungi on Plants in Brazil*. Embrapa. https://pragawall.cenargen.embrapa.br/aiqweb/michtml/fgbanco01.asp.

Farr, D. F., A. Y. Rossman, and L. A. Castlebury. 2026. *United States National Fungal Databases*. USDA ARS Mycology and Nematology Genetic Diversity and Biological Laboratory. https://fungi.ars.usda.gov.

Gao, Y., C. Ren, Y. Liu, et al. 2021. "Pepper–Maize Intercropping Affects the Occurrence of Anthracnose in Hot Pepper." *Crop Protection* 148: 105750.

Guarnaccia, V., I. Martino, G. Gilardi, A. Garibaldi, and M. L. Gullino. 2021. "*Colletotrichum* spp. Causing Anthracnose on Ornamental Plants in Northern Italy." *Journal of Plant Pathology* 103: 127–137.

He, Y., C. Shu, J. Chen, and E. Zhou. 2014. "First Report of Anthracnose of *Alocasia macrorrhiza* Caused by *Colletotrichum karstii* in Guangdong, China." *Plant Disease* 98: 696.

Hepperle, D. 2021. *SeqAssem—Contig Sequence Assembly Software*. SequentiX - Digital DNA Processing.

Hou, L. W., F. Liu, W. J. Duan, and L. Cai. 2016. "*Colletotrichum aracearum* and *C. camelliae-japonicae*, Two Holomorphic New Species From China and Japan." *Mycosphere* 7: 1111–1123.

Huang, R., W. Sun, W. Li, et al. 2021. "First Report of *Colletotrichum siamense* Causing Leaf Spot on *Alocasia macrorrhiza* in China." *Plant Disease* 105: 1857.

Huson, D. H., and D. Bryant. 2024. "The SplitsTree App: Interactive Analysis and Visualization Using Phylogenetic Trees and Networks." *Nature Methods* 21: 1773–1774.

Jayawardena, R. S., K. D. Hyde, Y. J. Chen, et al. 2020. "One Stop Shop IV: Taxonomic Update With Molecular Phylogeny for Important Phytopathogenic Genera: 76–100 (2020)." *Fungal Diversity* 103: 87–218.

Johnston, P. R., and D. Jones. 1997. "Relationships Among *Colletotrichum* Isolates From Fruit-Rots Assessed Using rDNA Sequences." *Mycologia* 89: 420–430.

Kumar, S., G. Stecher, M. Li, C. Knyaz, and K. Tamura. 2018. "MEGA X: Molecular Evolutionary Genetics Analysis Across Computing Platforms." *Molecular Biology and Evolution* 35: 1547–1549.

Lecomte, C., C. Alabouvette, V. Edel-Hermann, F. Robert, and C. Steinberg. 2016. "Biological Control of Ornamental Plant Diseases Caused by *Fusarium oxysporum*: A Review." *Biological Control* 101: 17–30.

Liu, F., Z. Y. Ma, L. W. Hou, et al. 2022. "Updating Species Diversity of *Colletotrichum*, With a Phylogenomic Overview." *Studies in Mycology* 101: 1–56.

Liu, Y., T. Cai, Q. Su, et al. 2024. "The Origin, Germplasm Resources, and Breeding of *Anthurium andraeanum*: An Overview." *Ornamental Plant Research* 2025, no. 1: e00353.

Liu, Y. L., J. R. Tang, and Y. H. Zhou. 2021. "First Report of *Colletotrichum siamense* Causing Anthracnose of *Monstera deliciosa* in Zhanjiang, China." *Plant Disease* 105: 1192.

Ma, X., S. Nontachaiyapoom, R. S. Jayawardena, et al. 2018. "Endophytic *Colletotrichum* Species From *Dendrobium* spp. in China and Northern Thailand." *MycoKeys* 43: 23–57.

Mariano, R. L. R., A. R. Peixoto, V. T. Holanda, S. M. A. Oliveira, and M. Menezes. 1989. "Doenças de plantas ornamentais no estado de Pernambuco." *Fitopatologia Brasileira* 14: 155.

Miller, M. A., W. Pfeiffer, and T. Schwartz. 2010. "Creating the CIPRES Science Gateway for Inference of Large Phylogenetic Trees." In *2010 Gateway Computing Environments Workshop (GCE)*, 1–8. IEEE.

Mmbando, G. S. 2023. "The Recent Relationship Between Ultraviolet-B Radiation and Biotic Resistance in Plants: A Novel Non-Chemical Strategy for Managing Biotic Stresses." *Plant Signaling & Behavior* 18: 2191463.

Müller-Xing, R., Q. Xing, and J. Goodrich. 2014. "Footprints of the Sun: Memory of UV and Light Stress in Plants." *Frontiers in Plant Science* 5: 108523.

Ning, P., M. Lu, L. Ma, and T. Deng. 2022. "First Report of Leaf Spot Caused by *Colletotrichum siamense* on *Philodendron bipinnatifidum* in Guangxi, China." *Plant Disease* 106: 1293.

Ningen, S. S., J. C. Cole, M. W. Smith, D. E. Dunn, and K. E. Conway. 2005. "Increased Shade Intensity and Afternoon Irrigation Decrease Anthracnose Severity on Three *Euonymus fortunei* Cultivars." *Hortscience* 40: 111–113.

Norman, D. J., and G. S. Ali. 2012. "Anthurium Diseases: Identification and Control in Commercial Greenhouse Operations." *EDIS* 4: 1–7.

Norphanphoun, C., J. P. Wang, X. C. Wang, H. D. Aumentado, F. Q. Liu, and Y. Wang. 2025. "Two New Species of *Colletotrichum* (Glomerellaceae, Glomerellales) and a New Host Record for *Colletotrichum karsti* on *Rosa chinensis* From Southwestern China." *MycoKeys* 122: 293–319.

Paz, C. D., A. R. P. Nascimento, B. R. Silva, et al. 1998. "Levantamento de doenças em plantas ornamentais no Médio São Francisco." *Fitopatologia Brasileira* 23: 329.

Pereira, C. M., E. C. d. A. Furtado, and R. W. Barreto. 2024. "Insights Into the Identity and Infectivity of the Fungi Causing *Cercospora* Leaf Spots on Two Ornamental Aroids in Brazil." *Journal of Phytopathology* 172: e13346.

Prasad, L., S. Javeria, B. Kumar, and P. Sharma. 2017. "First Report of Anthracnose of Elephant Foot Yam Caused by *Colletotrichum siamense* in India." *New Disease Reports* 36: 21.

Rayner, R. W. 1970. *A Mycological Colour Chart*. Mycological institute and British Mycological Society.

Ronquist, F., M. Teslenko, P. Van Der Mark, et al. 2012. "MrBayes 3.2: Efficient Bayesian Phylogenetic Inference and Model Choice Across a Large Model Space." *Systematic Biology* 61: 539–542.

Schoch, C. L., K. A. Seifert, S. Huhndorf, et al. 2012. "Nuclear Ribosomal Internal Transcribed Spacer (ITS) Region as a Universal DNA Barcode Marker for Fungi." *Proceedings of the National Academy of Sciences of the United States of America* 109: 6241–6246.

Silva, A. L., S. Salcedo-Sarmiento, P. S. C. Mansur, and R. W. Barreto. 2021. "*Colletotrichum karstii* Causes Anthracnose on the Orchid *Cattleya walkeriana* in Brazil." *Australasian Plant Disease Notes* 16: 18.

Silva-Cabral, J. R. A., J. L. da Silva, L. d. S. H. Soares, et al. 2019. "First Report of *Colletotrichum fructicola* and *C. tropicale* Causing Anthracnose on Orchids in Brazil." *Plant Disease* 103: 2672.

Smith, B. J., E. T. Stafne, H. F. Sakhanokho, and B. J. Sampson. 2023. "Intensity of Supplemental Greenhouse Lighting Affects Strawberry Plant Growth, Anthracnose Infection Response, and *Colletotrichum* Pathogen Development in Culture." *Hortscience* 58: 127–133.

Stamatakis, A. 2014. "RAxML Version 8: A Tool for Phylogenetic Analysis and Post-Analysis of Large Phylogenies." *Bioinformatics* 30: 1312–1313.

Stöver, B. C., and K. F. Müller. 2010. "TreeGraph 2: Combining and Visualizing Evidence From Different Phylogenetic Analyses." *BMC Bioinformatics* 11: 7.

Talhinhas, P., and R. Baroncelli. 2021. "*Colletotrichum* Species and Complexes: Geographic Distribution, Host Range and Conservation Status." *Fungal Diversity* 110: 109–198.

Talhinhas, P., and R. Baroncelli. 2023. "Hosts of *Colletotrichum*." *Mycosphere* 14: 158–261.

Tao, G., Z.-Y. Liu, F. Liu, Y.-H. Gao, and L. Cai. 2013. "Endophytic *Colletotrichum* Species From *Bletilla ochracea* (Orchidaceae), With Descriptions of Seven New Species." *Fungal Diversity* 61: 139–164.

Tennakoon, D. S., C.-H. Kuo, S. S. N. Maharachchikumbura, et al. 2021. "Taxonomic and Phylogenetic Contributions to *Celtis formosana*, *Ficus ampelas*, *F. septica*, *Macaranga tanarius* and *Morus australis* Leaf Litter Inhabiting Microfungi." *Fungal Diversity* 108: 1–215.

Tinyane, P. P., P. Soundy, and D. Sivakumar. 2018. "Growing 'Hass' Avocado Fruit Under Different Coloured Shade Netting Improves the Marketable Yield and Affects Fruit Ripening." *Scientia Horticulturae* 230: 43–49.

Vaidya, G., D. J. Lohman, and R. Meier. 2011. "SequenceMatrix: Concatenation Software for the Fast Assembly of Multi-Gene Datasets With Character Set and Codon Information." *Cladistics* 27: 171–180.

Vanhaelewyn, L., D. Van Der Straeten, B. De Coninck, and F. Vandenbussche. 2020. "Ultraviolet Radiation From a Plant Perspective: The Plant-Microorganism Context." *Frontiers in Plant Science* 11: 597642.

Vásquez-López, A., R. E. Palacios-Torres, M. Camacho-Tapia, et al. 2019. "*Colletotrichum brevisporum* and *C. musicola* Causing Leaf Anthracnose of Taro (*Colocasia esculenta*) in Mexico." *Plant Disease* 103: 2963.

Vieira, W. A. d. S., P. A. Bezerra, A. C. da Silva, J. S. Veloso, M. P. S. Câmara, and V. P. Doyle. 2020. "Optimal Markers for the Identification of *Colletotrichum* Species." *Molecular Phylogenetics and Evolution* 143: 106694.

Visagie, C. M., N. Yilmaz, J. D. Allison, et al. 2024. "New and Interesting Fungi. 7." *Fungal Systematics and Evolution* 13: 441–494.

Vithanage, I. S. K., D. M. D. Yakandawala, S. S. N. Maharachchikumbura, L. Jayasinghe, and N. K. B. Adikaram. 2021. "*Colletotrichum* Species Causing Anthracnose Disease in *A. andraeanum*, Manifested as Spathe Rot Also in Addition to Spadix Rot and Leaf Spot." *European Journal of Plant Pathology* 161: 837–846.

Wang, R., D. Ouyang, M. Lu, et al. 2024. "Identification and Characterization of *Colletotrichum* Species Associated With Anthracnose Disease of Plum." *Plant Disease* 108: 2874–2886.

Wu, F., S. C. Li, Y. B. Wang, et al. 2022. "First Report of *Colletotrichum karsti* Causing Anthracnose of *Begonia lanternaria* in China." *Plant Disease* 106: 2990.

Xue, L., Y. Zhang, T. Duan, et al. 2020. "Characterization and Pathogenicity of *Colletotrichum* Species on *Philodendron tatei* cv. Congo in Gansu Province, China." *Plant Disease* 104: 2571–2584.

Yang, Y., L. Cai, Z. Yu, Z. Liu, and K. D. Hyde. 2011. "*Colletotrichum* Species on Orchidaceae in Southwest China." *Cryptogamie, Mycologie* 32: 229–253.

Ye, R., G. Shao, Z. Ma, Q. Gao, B. Wang, and T. Li. 2024. "Prediction of Anthracnose Risk in Large-Leaf Tea Trees Based on the Atmospheric Environmental Changes in Yunnan Tea Gardens—Cox Regression Model and Machine Learning Model." *Agronomy* 14: 1501.

Zapata, M., E. Rodríguez-Serrano, J. F. Castro, et al. 2024. "Novel Species and Records of *Colletotrichum* Associated With Native Woody Plants in South-Central Chile." *Mycological Progress* 23: 18.

Zhai, Y. X., B. Q. Zhang, H. Cao, and X. J. Hao. 2018. "First Report of *Colletotrichum truncatum* Causing Anthracnose of Begonia in China." *Plant Disease* 102: 1177.

Zhang, Q., M. M. Nizamani, Y. Feng, et al. 2023. "Genome-Scale and Multi-Gene Phylogenetic Analyses of *Colletotrichum* spp. Host Preference and Associated With Medicinal Plants." *Mycosphere* 14: 1–106.

Zhang, Y., J. Chen, I. Manawasinghe, et al. 2023. "Identification and Characterization of *Colletotrichum* Species Associated With Ornamental Plants in Southern China." *Mycosphere* 14: 262–302.

Zheng, H., Z. Yu, X. Jiang, L. Fang, and M. Qiao. 2022. "Endophytic *Colletotrichum* Species From Aquatic Plants in Southwest China." *Journal of Fungi* 8: 87.

Supporting Information

Additional supporting information can be found online in the Supporting Information section. **Table S1:** ppa70178-sup-0001-TableS1.docx. *Colletotrichum* species, culture number, information and GenBank accession numbers for strains used in the phylogenetic trees. **Table S2:** Primers used in this study, with DNA sequences, annealing temperatures and times and references. **Figure S1:** Phylogenetic tree based on Bayesian inference analysis (BI) of the rDNA internal transcribed spacer region (ITS), glyceraldehyde 3-phosphate dehydrogenase (*gapdh*), chitin synthase 1 (*chs-1*), actin (*act*) and β-tubulin 2 (*tub2*) sequences of members of the *Colletotrichum* species complexes. Thickened branches indicate nodes with BI posterior probabilities values higher than 0.90. The tree is rooted with *Monilochaetes infuscans* (CBS 869.96). *Colletotrichum boninense* species complex is highlighted in green and isolates treated in this study are presented in red. **Figure S2:** Phylogenetic trees inferred from maximum-likelihood analyses based on individual loci (rDNA ITS, *gapdh*, *chs-1*, *act*, *tub2*, *his3* and *cal*) of members of the *Colletotrichum boninense* species complex. Bootstrap support higher than 70% are shown above the nodes. Isolates included in this study are highlighted in red. **Figure S3:** Phylogenetic tree based on Bayesian inference analysis (BI) and maximum-likelihood (ML) of the rDNA internal transcribed spacer region (ITS), glyceraldehyde 3-phosphate dehydrogenase (*gapdh*), chitin synthase 1 (*chs-1*), actin (*act*) and β-tubulin 2 (*tub2*) sequences of members of the *Colletotrichum boninense* species complex. Thickened branches indicate nodes with ML bootstrap support (BS) higher than 90% and BI posterior probabilities (PP) values higher than 0.95. Values at nodes indicate BS values (left, values ≥ 70%) and PP from BI (right, values ≥ 0.9). Lower values are indicated as '–'. The tree is rooted with *C. gloeosporioides* (CBS 112999 and CBS 953.97). Ex-type strains are highlighted in bold and isolates treated in this study are presented in red.